Hydrodynamic Study in the Bay of Calvi - Measurements and Analysis of Currents

Auteur : Cugerone, Claude
Promoteur(s) : Alvera Azcarate, Aida; Barth, Alexander
Faculté : Faculté des Sciences
Diplôme : Master en océanographie, à finalité approfondie
Année académique : 2024-2025
URI/URL : http://hdl.handle.net/2268.2/22284

Hydrodynamic Study in the Bay of Calvi Measurements and Analysis of Currents

Claude Cugerone

Master thesis written in order to obtain the degree of Master en Océanographie

Supervisors: Aïda Alvera-Azcarate - Alexander Barth
GeoHydrodynamics and Environment Research (GHER)
University of Liège.

January 17, 2025

Contents

List of Acronyms

ADCP Acoustic Doppler Current Profiler

AOT Autorisation d'Occupation Temporaire (Temporary Occupation Permit)

ECC Eastern Corsican Current

LPB Ligurian-Provence Basin

NC Northern Current

RCM Rotor Current Meter

SST Sea Surface Temperature

STARESO Station de Recherche Sous-marine et Océanographique

WCC Western Corsican Current

List of Figures

List of Tables

According to the rules imposed by the jury of the Master in Oceanography, this document must not exceed 50 pages in Times 12 or an equivalent font.

Remerciements

Avant de vous plonger dans la lecture de ce manuscrit, je souhaiterais remercier avec plus de légereté les personnes qui m'ont apporté aide et soutien lors de ce mémoire et durant cette aventure de deux ans.

Tout d'abord, je tiens à remercier mes promoteurs, les docteurs Aïda Alvera-Azcarate et Alexander Barth, pour leur soutien dans l'élaboration de ce manuscrit. Leur expertise et leur engagement ont su me guider et me fournir de bons conseils. Merci de m'avoir permis de participé aux réunions du GHER. J'ai beaucoup appris le peu de fois où j'ai pu y assister. Merci d'avoir également pris tant d'heures sur des sites de vente en ligne afin de trouver les pièces et outils indispensables à la réalisation des déploiements. Je suis profondément reconnaissant pour leur encadrement précieux qui a permis ce mémoire et enrichi ma compréhension du domaine.

Je tiens également à remercier mon comité de lecture, Aïda Alvera-Azcarate, Alexander BARTH, Sylvie Gobert, Charles Troupin et Anne Goffart, qui ont eu la patience de lire ces pages.

Un grand merci au personnel de STARESO, qui m'ont supporté 4 semaines durant en Corse, et qui ont eu la joie d'immerger des instruments pour moi. Leur expertise a été d'une grande aide, et la collaboration avec cette équipe à la fois passionnée et compétente était un réel plaisir. Un merci tout particulier à Lovina Fulgrabe, qui s'est chargée de m'envoyer toutes les données récoltées. Merci !

À Anna, Annabelle, Emmanuel, Théo, Delphine, Céline et Dodo. Cette aventure de 2 ans n'aurait pas été possible sans votre soutien. Un grand merci à vous !

À Gregoire, Clara, Valentin, Georges et Anthony, qui ont été les gardiens de ma santé mentale tout au long de l'écriture de ce mémoire. Leur capacité à détendre l'atmosphère avec des soirées de jeux de société et des "blagues" a été une bouffée d'air frais pendant les moments de stress intense.

Merci à Floriane, cela fait presque 20 ans que l'on se connait et tu as toujours été un soutien important dans ma vie, notamment lors de nos expériences Erasmus respectives. Nos visites respectives et nos voyages ensemble resteront dans ma mémoire à jamais. Merci pour ta bonne humeur, ta gentillesse, ton soutien constant et les raclettes que tu organises, même en été !

Merci à Cédric Delforge de m'avoir envoyé ses photos prises en baie de Calvi pour illustrer ce mémoire.

À mes relecteurs de première heure et de dernière minute, qui ont amélioré la qualité grammaticale et orthographique de ce mémoire de manière significative.

Hydrodynamic Study in the Bay of Calvi
Measurements and Analysis of Currents

Claude Cugerone

Résumé

Cette étude se concentre sur l'analyse des courants dans la baie de Calvi, en Corse, à l'aide de mesures obtenues grâce à des Acoustic Doppler Current Profilers (ADCP). La recherche inclut également le traitement et l'analyse de données historiques issues de campagnes précédentes. Ces ensembles de données ont été comparés aux mesures ADCP afin d'obtenir une compréhension des dynamiques des courants dans la région. L'objectif principal de l'étude était d'identifier les variations spatiales et temporelles des courants, ainsi que de comprendre les dynamiques principales des courants et leur évolution à la fois à court terme (annuellement) et à long terme (sur plusieurs années). L'étude a réussi à répondre à ces deux questions. D'une part, des variations spatiales et temporelles significatives des courants ont été observées. D'autre part, les dynamiques principales des courants se sont révélées changeantes, influencées par des processus à l'échelle mésoscalaire et à grande échelle, bien que ces processus n'aient pas pu être identifiés dans le cadre de cette étude. Sur plusieurs années, la tendance des dynamiques des courants est restée relativement stable à long terme, malgré des variations à petite échelle.

Hydrodynamic Study in the Bay of Calvi
Measurements and Analysis of Currents

Claude Cugerone

Abstract

This study focuses on the analysis of currents in Calvi Bay, Corsica, using measurements obtained through Acoustic Doppler Current Profilers (ADCPs). The research also includes the processing and analysis of historical data from previous campaigns. These datasets were compared to the ADCP measurements in order to achieve a comprehensive understanding of the current dynamics in the region. The main objective of the study was to identify spatial and temporal variations in the currents, and to understand the principal dynamics of the currents and their evolution over both short-term (yearly) and long-term (multi-year) scales. The study successfully addressed these two questions. First, significant spatial and temporal variations in the currents were observed. Second, the primary dynamics of the currents were found to be changeable, influenced by both mesoscale and large-scale processes, although those processes could not be identified within the scope of this study. Over multiple years, the current dynamics trend remained relatively stable on a long-term vision, despite smaller-scale variations.

1 Introduction

The Mediterranean Sea is a region of significant ecological, economic, and scientific importance for Europe. Its semi-enclosed nature and rapid water circulation—where waters complete a full cycle in approximately 75 years, compared to nearly 1,000 years in open oceans—make it particularly sensitive to environmental changes (Schroeder et al., 2012). This accelerated turnover renders the Mediterranean a hotspot for studying climate change and its impacts on marine ecosystems.

Within this context, the Bay of Calvi, located on the northwest coast of Corsica, serves as a strategic site for oceanographic research. It hosts the Station de Recherche Sous-marine et Océanographique (STARESO), which supports many projects related to oceanography, like the STARECAPMED project for instance, which aims to provide scientific data on the state, evolution, and processes of marine ecosystems, supporting informed decision-making for sustainable ocean management and policy development (Richir et al., 2015). The STARESO has a long tradition of conducting studies with ULiège (University of Liège), allowing students to analyze physico-chemical studies in the Bay of Calvi, monitoring the presence of microplastics in the water, or analyzing the hydrodynamics of the bay.

This study focuses on understanding the marine currents in the Bay of Calvi, which play a key role in the dynamics of local water masses and connect to the broader Ligurian Sea system. First, it presents the geographical and physical characteristics of the bay, followed by an exploration of the factors influencing marine currents. Finally, the study highlights the importance of analyzing these currents to better understand regional hydrodynamics and their implications.

1.1 Context and background

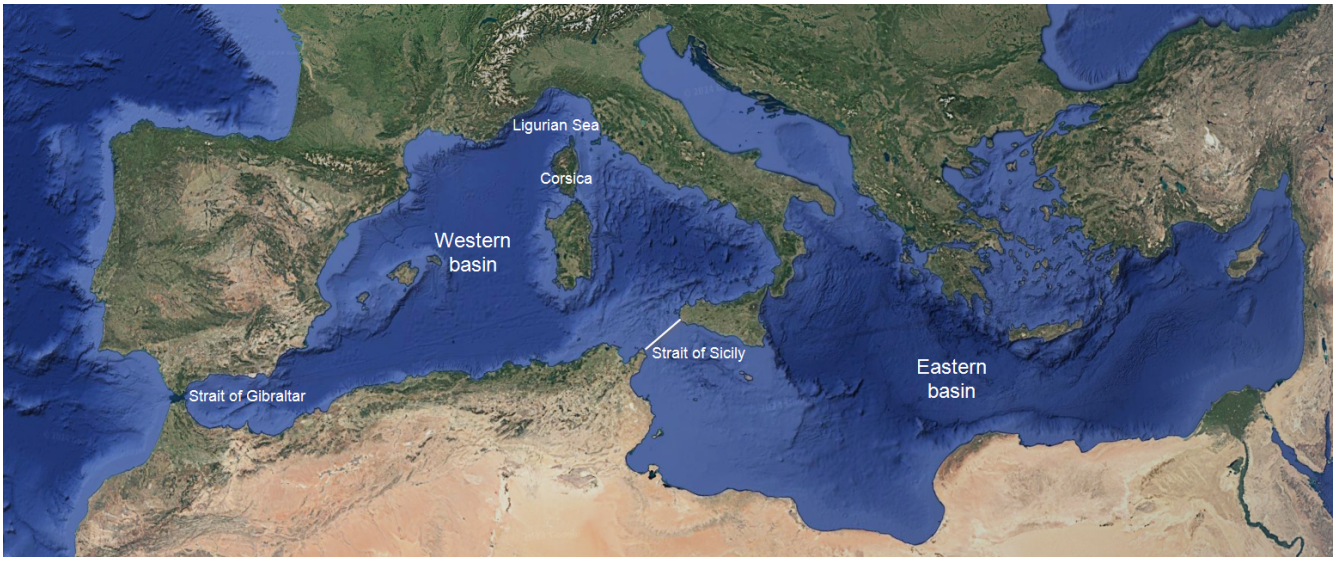

Figure 1: Overall of the key geographical features of the Mediterranean Sea (Google Earth).

Located in southern Europe, the Mediterranean Sea is found between 30 ° and 40 ° north latitude. It is a natural boundary between Europe and Africa. With an area of 2.54 million km², it has an average depth of 1500 meters and is nearly landlocked. Its only connection to the open ocean is the Strait of Gibraltar.

The Mediterranean is divided into two primary basins: the western and eastern Mediterranean. The Strait of Sicily, situated between Tunisia and Sicily (figure 1), serves as the dividing line between these two basins (Viollette, 1994).

1.1.1 The Ligurian Sea

The Ligurian Sea is part of the western Mediterranean Sea, located between the northwestern coast of Italy and the island of Corsica. Bordered by the regions of Liguria in Italy to the east and Provence-Alpes-Côte d'Azur in France to the west, this sea is known for its deep waters and relatively narrow coastal shelf.

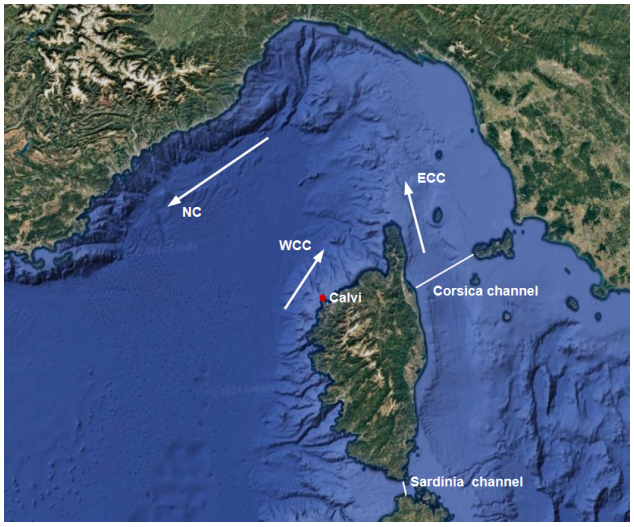

Figure 2: The Ligurian Sea, illustrated with the three major currents: Eastern Corsican Current (ECC), Western Corsican Current (WCC) and Northern Current (NC) (Barth et al., 2005) (Google Earth).

Three major currents can be identified within the Ligurian Sea (figure 2) : the Eastern Corsican Current (ECC), the Western Corsican Current (WCC) and the Northern Current (NC) (Barth et al., 2005). The circulation in the Ligurian-Provence Basin (LPB) is connected to the Tyrrhenian and Balearic seas by two currents that flow north on either side of Corsica. The ECC brings water from the Tyrrhenian Sea into the LPB (Astraldi et al., 1990). This movement occurs due to a difference in sea level between the Tyrrhenian Sea and the LPB, which is strongest in winter when the basin loses more heat. The wind plays a role in driving this current. Without wind, the flow through the Corsica channel weakens a lot and, in summer, the current can even reverse direction (Poulain et al., 2012).

West of Corsica, the other current is the WCC, which stays steady throughout the year. This current is part of a large swirling system in LPB. It is mainly influenced by the formation of dense water during winter in the central LPB and the dominant winds from the northeast such as Mistral and Tramontane (Poulain et al., 2012). Driven by the wind, the ECC and WCC meet north of Corsica, and form the NC. This stronger current flows along the coasts of western Italy, France, and Spain. Its speed can reach up to 1 meter per second at the surface and about 5 centimeters per second at 400 meters depth, with speeds decreasing in the summer (Poulain et al., 2012).

1.1.2 Corsica

Corsica is an island located in the Mediterranean Sea, southeast of France and west of Italy. It is located in the LPB and impacted by the NC (Poulain et al., 2012). Corsica is also bordered by the Corsica channel and the Sardinia channel, which respectivelly separates it from Italy to the east and from Sardinia to the south (figure 2). This geographical position gives Corsica a Mediterranean climate with significant maritime influences. The island is composed of interior mountains which dominate the island landscape, allowing for a river system coming from the mountains (Gobert et al., 2018). This one is composed of a multitude of small rivers, characterized by two periods of high water and two periods of low water. In the bay of Calvi, the two main rivers are the Figarella and the Fiume Seccu. During autumn storms, their flow rates generally reach maximum values, varying considerably throughout the year.

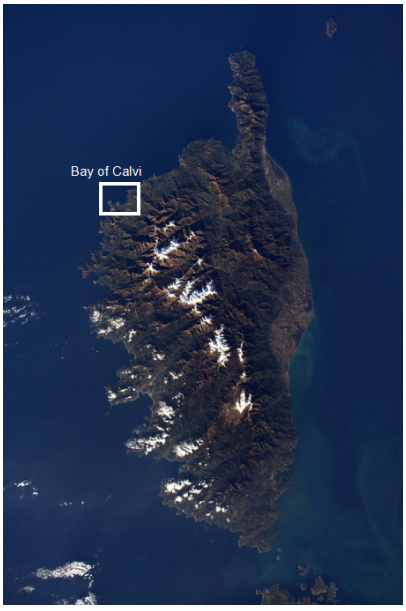

(a) Picture of Corsica from the International Space Station.

(b) Satellite image of the Calvi Bay.

Figure 3: (a) True-color image of Corsica taken from the International Space Station by Thomas Pesquet. Credits: ESA/NASA. (b) Close-up of the Bay of Calvi, taken from Google Earth. The Bay of Calvi is highlighted with a white rectangle on image (a).

1.1.3 The Bay of Calvi

The Bay of Calvi (42°34'N 8°45'E) is situated in the Balagne region, in the northwest of Corsica (figure 3 (a)). With an area of 22.26 km², the bay is bordered to the north by a 6.3 km wide opening between Punta de la Revellata and Punta di Spanu. It is divided into two smaller water bodies: the Bay of Revellata to the west and the Gulf of Calvi to the east (figure 3 (b)).

The physical characteristics of the bay is typical of the Mediterranean Sea. The tidal range is low and does not exceed 10 centimeters. The salinity is around 38 in the upper layer. The water temperature varies between 12 and 26°C. A thermocline forms during the summer months at a depth of approximately 25-30 meters from May to October but dissipates during winter (Remy, 2016).

Water circulation in the bay is complex and influenced by external hydrodynamic factors. The Liguro-Provençal front and the winds strongly impact the water bodies in the bay. The identification of a double gyre circulation pattern has been described by Norro (1995): an anticyclonic gyre (clockwise rotation in the Northern Hemisphere) in the western part and a cyclonic gyre (anti-clockwise rotation) in the eastern part, but the presence of a single anticyclonic gyre has been occasionally observed too. Upwellings were also observed when winds blew from the northeast. This deep water originates from a submarine canyon located 3 km offshore. Its head (or mouth) is situated in front of the Bay of Calvi (Norro, 1995).

The Canyon of Calvi (42°38'N, 8°42'E), with an average depth of 600 meters, has a maximum depth of 1000 meters, 10 km offshore (Lepoint, 2001). It plays an important role in the exchange of water, sediments, and other materials happening between the continental shelf and the submarine slope (Skliris et al., 2002). As long as water masses remain outside of the submarine canyon, the current near the Bay of Calvi stays in a near-geostrophic balance, following isobaths with minimal cross-shelf exchanges. However, the hydrodynamic circulation is disturbed if water masses cross the canyon. Skliris et al. (2001) demonstrates that circulation from or towards the canyon is mainly related to wind. With a simplified model, it is reported that wind forcing during the storm leads to a significant increase in both cross-shore and vertical transports in the region. The simulation reveals strong downwelling throughout the continental slope. The study also confirms that the current within the Bay of Calvi depends on the circulation pattern around the canyon, offshore of the bay (Skliris et al., 2001).

1.1.4 Seasonal variations

Weather plays a crucial role on the hydrodynamic circulation within the LPB. Cold land-based winds during winter, such as the Mistral and Tramontane, create significant temperature and water gradients by extracting heat from the basin. This gradient intensifies from October to December and then decreases in February. Atmospheric-climatic conditions in winter have been identified as the main factors impacting the basin circulation (Astraldi et al., 1994). These conditions generate different thermohaline properties in the LPB, becoming a spot for deep water formation during winter. A study has also highlighted that the current velocity along the western side of Corsica peaks in early summer, driven by deep water formation (Astraldi et al., 1994). This corresponds to the seasonal increase of the WCC indicated by the Princeton Ocean Model (Ahumada and Cruzado, 2007). The WCC current is the least active during late summer and autumn, and remains weaker than the ECC. The ECC transport decreases in winter. This current is mainly impacted by atmospheric conditions and water differences between the western and the eastern part of the Mediterranean Sea (Echevin et al., 2003). The NC resulting from a combination of the ECC and the WCC, depicts also a seasonality in summer: during this period, it is almost exclusively composed of water coming from the western side of Corsica.

Results from the Princeton Ocean Model indicate that in the northern part of the northwestern Mediterranean, the large-scale cyclonic circulation is less consistent in winter and spring compared to its coherent behavior during summer and autumn, especially in the upper layers (Ahumada and Cruzado, 2007).

1.1.5 Marine currents

To fully understand the marine currents of the Bay of Calvi, it is essential to examine the phenomena that influence them. Ocean currents, such as the Gulf Stream, are well known to the general public and play a crucial role in regulating the global climate and transporting heat across the oceans (Minobe et al., 2008). Essential to marine dynamics, ocean currents are continuous, directed movements of water driven by various forces (Beesley et al., 2008). Their direction and strength are shaped by a complex combination of factors. Some of them are outlined below.

Density

Variations in water temperature, salinity, and pressure affect water density, creating different layers of water that overlap. The density of seawater depends primarily on these three factors:

- Temperature: Colder water is denser than warmer water because water contracts as it cools, increasing its density.
- Salinity: Saltier water is denser than fresh water due to the added mass of dissolved salts. This makes salinity a key factor in determining water density.
- Pressure: Increased pressure at greater depths compresses water slightly, making it denser. However, this effect is generally less significant compared to temperature and salinity.

These variations in density are responsible for several hydrodynamic processes and phenomena. Fronts can form at the boundaries between water masses with different densities, leading to sharp changes in temperature, salinity, and density over short distances. Also, vertical mixing occurs as denser water sinks beneath less dense water, driving circulation patterns and promoting nutrient exchange between layers. The movement and mixing of water driven by density differences play a fundamental role in global ocean dynamics, including the thermohaline circulation, which redistributes heat and nutrients across the planet (Minobe et al., 2008).

Coriolis force

The Coriolis force significantly impacts the movement of ocean currents and atmospheric winds at the scale of an ocean basin. It is an apparent force that results from the Earth's rotation and acts in a rotating reference frame. The Earth's angular velocity is constant, but the Coriolis effect depends on latitude, being zero at the equator and reaching its maximum at the poles. This dependence on latitude causes moving objects to appear deflected to the right in the Northern Hemisphere and to the left in the Southern Hemisphere.

Unlike gravitational effects that also influence trajectories, such as parabolic paths observed in an inertial frame, the Coriolis force specifically results from Earth's rotation. It plays a key role in shaping large-scale ocean currents and atmospheric circulation patterns, including winds, cyclones, and gyres.

The Coriolis Force F_c is given by the equation:

$$\mathbf{F_c} = -2\Omega \wedge \mathbf{u} \tag{1}$$

where Ω is the Earth's angular rotation rate, and $\mathbf{u}$ is the current velocity vector.

A simple way of describing this equation is that the Coriolis force acts perpendicular to the direction of motion, deflecting winds and currents.

The Coriolis frequency, often denoted by f, is related to the Coriolis force and reflects the Coriolis force effect based on latitude. It is given by the following equation:

$$f = 2\Omega \sin(\phi) \tag{2}$$

where ϕ is the latitude. This equation shows that the Coriolis force (acting in the horizontal plane) is zero at the equator and reaches its maximum near the poles, meaning there is no deflection at the equator and the strongest deflection occurs near the poles: to the right in the Northern Hemisphere and to the left in the Southern Hemisphere, due to the negative sign of $\sin(\phi)$.

The influence of the Coriolis force on ocean currents was first identified by Norwegian scientist and explorer Fridtjof Nansen (1861–1930). During an Arctic expedition in 1893, Nansen observed that ice and his ship, Fram, drifted at an angle of 20°–40° to the right of the wind direction. He shared this observation with Vilhelm Bjerknes, who later tasked his student V. Wilfrid Ekman to develop a theoretical explanation. In 1905, Ekman described the mechanism of wind-driven currents deflected by the Coriolis force, now known as Ekman currents (Beesley et al., 2008).

Ekman Transport

When wind blows over the ocean surface, it drags the water with it due to friction. However, because of the Coriolis effect, the surface water is deflected at an angle to the direction of the wind, with the direction of deflection depending on the hemisphere. It gets deflected to the right in the northern Hemisphere and to the left in the southern Hemisphere. The deflection propagates in the different layers of the water column.

Shoreline configurations and other geographical features also influence the currents. Coupled with Ekman transport, these features can significantly impact coastal environment. When winds blow along the coast, the direction of the winds determines the type of water movement. If the winds blow offshore, surface water is pushed away and replaced by deep water, leading to upwelling. If the winds blow onshore, surface water is pushed toward the coast, leading to downwelling (D. Wang et al., 2013).

Together, all these factors create diverse water movements, impacting the transport of heat and planktonic organisms. Indeed, marine currents also help in predicting the "horizontal migration" of planktonic organisms and the plankton dispersal, enhancing our understanding of species distribution, their adaptation to environmental changes (Goffart et al., 2002), and their roles in marine ecosystems. The transport of

suspended sediment is highly influenced by both particle size and current velocity (Van Rijn, 2007), as well as pollutant transport dynamics, including plastic waste, which can travel far away before accumulating in ocean gyres like the Pacific's infamous "seventh continent" of waste (Law et al., 2010).

1.2 Importance of studying marine currents in Calvi Bay

1.2.1 Applications of current measurements

Analyzing these phenomena and understanding the marine currents of the Bay of Calvi is crucial, as it helps to understand their impact on the ecosystem and human activities. This can provide critical data for various applications. It assists in the safe and efficient movement of vessels, contributing significantly to navigation. Moreover, it plays a crucial role in environmental studies, helping in the monitoring and preservation of marine ecosystems. Sedimentation studies benefit from this data by enhancing our understanding of sediment transport and deposition, which is also necessary to understand coastal erosion. Additionally, by comprehending sediment dynamics, the need for dredging harbors can be reduced. Studying marine currents also facilitates the analysis of horizontal migration patterns of marine species and tracks the dispersion of pollutants and nutrients in the water, thereby providing valuable insights on pollutant and nutrient transport (Williams and Follows, 2003). These applications highlight the importance of current measurements for sustainable marine and coastal management.

1.2.2 Main objectives of the study and specific research questions

Since 2018, no current measurement campaigns have been conducted into the bay of Calvi. A comprehensive analysis that brings together all available data, despite their temporal and spatial disparities, is lacking in order to establish the dominant patterns and scales of current variability. The main objective of this study is to conduct a review of the currents in Calvi Bay by integrating both historical and new data. To achieve this, the study gathered existing data on marine currents collected by previous campaigns, including records from 1998 to 2002 and from 2015 to 2018. In addition to these data, a current measurement campaign has also been conducted on different sites within the bay from September 2023 to April 2024. This allows to compare current variations over time and obtain a detailed overview of the bay's current dynamics. Specifically, the study aims to address two key questions: "What are the temporal and spatial variations of the currents in Calvi Bay across the different periods and observation sites?" and "What are the main dynamics of the currents in Calvi Bay, and how have these dynamics evolved between the measurement periods (1998–2002, 2015–2018, 2023–2024)?" These questions will guide the analysis and comparison of historical and recent data, providing insights into the current dynamics in Calvi Bay and their variations over time and space.

The study helps identify changes in current tendencies over the years or months, and provide a basis for future research. Indeed, these results can be used to target specific under-sampled or under-observed areas where currents are still poorly understood, facilitating more focused and detailed future studies.

Additionally, these information can be helpful for bay management and conservation of local marine resources. Like in many scientific currents measuring campaigns, an ADCP (Acoustic Doppler Current Profiler) is used (Kostaschuk et al., 2005). The measurement campaign is completed with the collaboration of the STARESO, located near Calvi. This partnership has allowed a use of their facilities and expertise in the field.

2 Methodology

This section outlines the methodology used during the sampling campaign. After a quick overview about ADCP, the section covers the sites studied within the bay, how ADCP operates and its configuration, the procedures for deployment and recovery, data collection and processing.

2.1 Instrumentation and equipment

Figure 4: The ADCPs used during the study: Seaguard type II from Aanderaa.

2.1.1 ADCP overview

An ADCP is an instrument that measures the speed and direction of ocean currents. There are different types of ADCPs designed to suit different measurement needs. Surface-mounted ADCPs are deployed on buoys or vessels to measure currents from the water's surface, while bottom-mounted ADCPs are placed on the seabed to monitor currents throughout the entire water column. ADCPs can also be either fixed, providing continuous data at a specific location, or mobile, where they are attached to moving platforms like ships or gliders, allowing for the measurement of current profiles over a larger area (Nortek, 2021). The instruments we use for this measurement campaign are bottom-mounted fixed.

The ADCP indirectly measures the speed of the water. Indeed, it measures the velocity of particles moving in water, such as plankton, suspended sediments in the water column, aggregated particles, etc. The particle is considered to have the same velocity as water. The ADCP emits an acoustic signal through a beam and measures the returning echo. By analyzing the Doppler effect in the echoed signal, it is possible to determine the velocity of the particles, which leads to the velocity of the water.

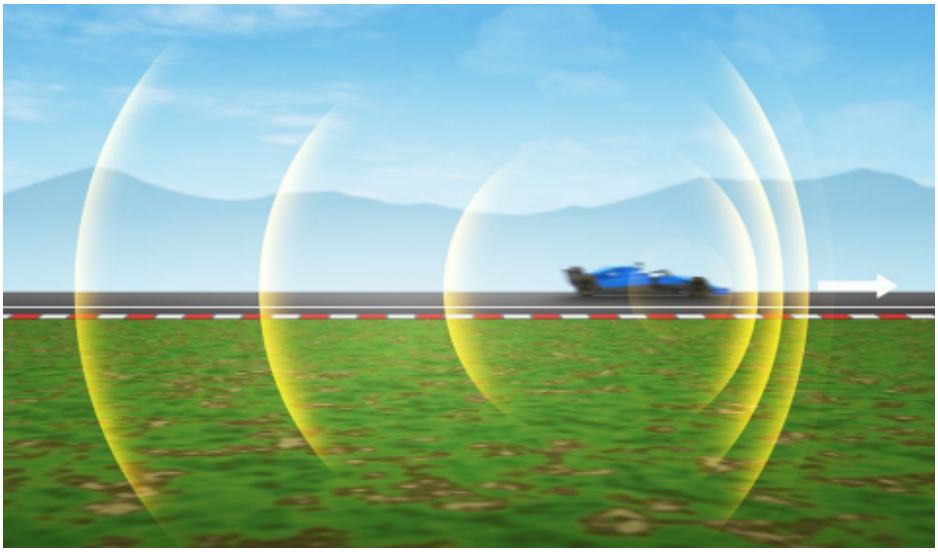

Figure 5: As the vehicle comes to the observer, all the sounds emitted by the formula 1 are compressed, resulting in a higher pitch (image from Nortek, 2021).

Doppler effect

The Doppler effect, also known as the Doppler shift, describes an alteration in the observed frequency of a sound when the source or the observer is moving. An everyday example of this effect is for instance the changing pitch of an ambulance siren coming at an observer. First, the ambulance siren emits a higher frequency as it comes to the observer, and then the frequency decreases as the vehicle goes away. This effect occurs because sound behaves as a wave. If the source moves towards the observer and generate waves, these are compressed, leading to a higher pitch, which means a higher frequency (figure 5). In contrast, if the source moves away from the observer, the waves are stretched, resulting in a lower pitch: a lower frequency.

To understand this phenomena, it is important to consider that the sound emitted at one point will propagate from this origin point, and that the source emits waves at a certain frequency with a constant wavelength (the ambulance siren is a perfect example). The figure 6 (from Moebs et al., 2023) illustrates this source moving. The wavelength λ_s emitted by the source and the frequency f_s are constant and we can observe the compression of the waves towards Y and their stretching towards X. Let λ_o being the wavelength the observer hears:

$$\lambda_o = \lambda_s \pm \Delta_x. \tag{3}$$

Δ_x represents the change in wavelength induced by the relative motion between the source and the observer.

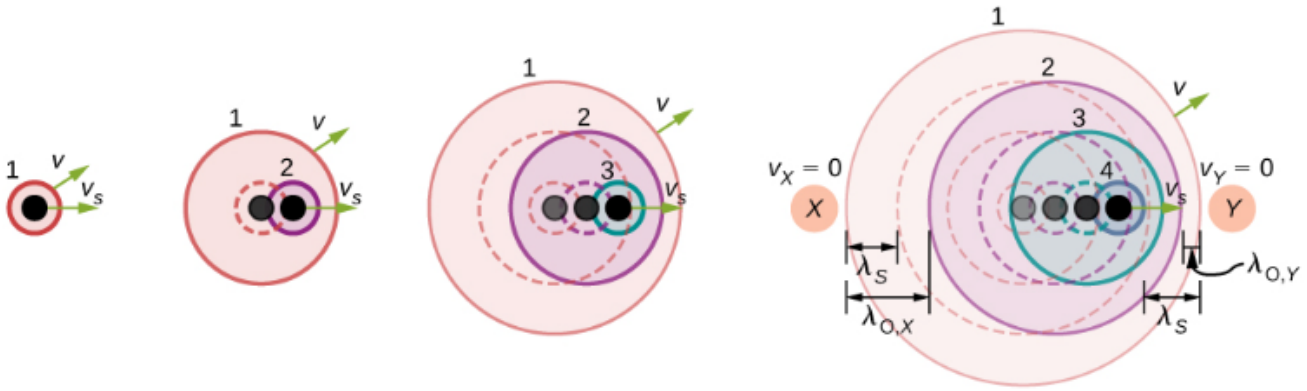

Figure 6: A source moving from a stationary observer at position X ($v_x = 0$) to a stationary observer at position Y ($v_y = 0$) at a constant speed v_s. Sounds waves are emitted by the black dot at a constant frequency f_s, with a constant wavelength λ_s, at the speed of sound v. The solid lines indicate the position of the sound waves at the initial time. The dotted lines represent the positions of the waves at each individual time period (Moebs et al., 2023).

As $\lambda = vT$, with v the phase velocity of the sound wave, T the period, which is the inverse of the frequency $T = \frac{1}{f_o}$, and $\Delta_x = v_s T_s$ (Urone and Hinrichs, 2020), equation 3 can be written as follows:

$$vT_o = vT_s \pm v_s T_s \tag{4}$$

$$\frac{v}{f_o} = \frac{v}{f_s} - \frac{v_s}{f_s} = \frac{v \pm v_s}{f_s} \tag{5}$$

$$f_o = f_s \left(\frac{v}{v \pm v_s} \right) \tag{6}$$

where f_o is the frequency observed by the stationary observer and f_s is the frequency produced by the moving source. The observed frequency f_o changes depending on the direction of motion of the source, with f_o increasing when the source moves towards the observer and decreasing when it moves away.

The sign $+$ or $-$ in the denominator depends on the direction of the relative motion of the source with respect to the observer. When the source approaches the observer, the observed frequency f_o increases. The $-$ sign is used in the denominator because the source velocity v_s reduces the distance between the source and the observer. When the source moves away from the observer, the observed frequency f_o decreases. The $+$ sign is used in the denominator because the source velocity v_s increases the distance between the source and the observer.

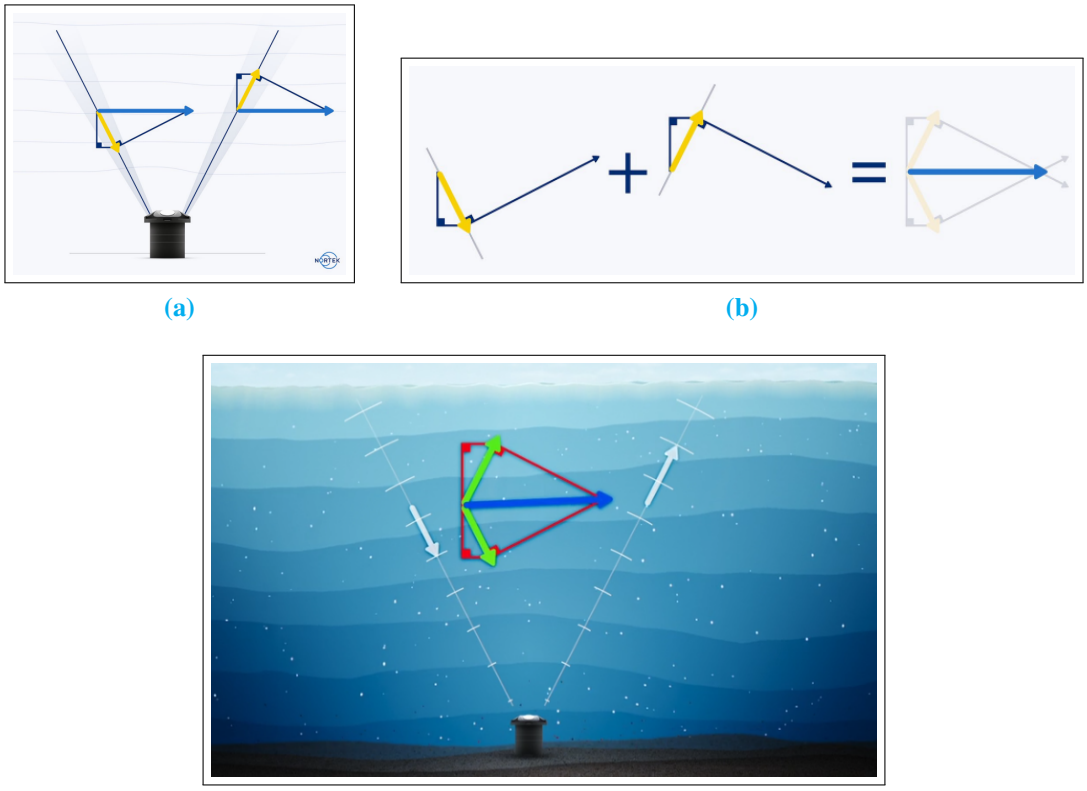

Figure 7: (a) The velocity is measured by a pair of beams oriented left and right. The water velocity is illustrated by the blue arrows, which is consistent for both beams. Each beam measures the component of this water velocity along its direction, represented by the yellow arrows. (b) By drawing lines perpendicular to the extremity of the two vectors, we obtain the water velocity and direction. (c) presents a summary of (a) and (b). (image from Nortek, 2021).

This effect can be observed in any type of wave, including acoustic, light, and other electromagnetic waves. ADCPs operate using acoustic waves in the 100 kHz to 2000 kHz range, depending on the desired ratio between range and resolution. Lower frequencies provide greater range but lower resolution, while higher frequencies offer better resolution at the cost of reduced range. ADCPs rely on the Doppler effect to measure distances based on echoes from suspended particles and compute water velocity. The ADCP emits an acoustic signal and measures the frequency of the reflected echo to determine the speed of the currents. If the water particles move relative to the instrument, the echo frequency will be shifted due to the Doppler effect. Using the frequency difference between the transmitted and received signals, one can calculate the component of the current velocity along the acoustic beam direction. This measurement is then used to estimate the speed of currents in the water (figure 7 (a)).

The ADCPs are equipped with several beams. With only one beam, we can only extract the vertical velocity of the particle relative to the beam. Water velocity can be computed, represented as the blue arrow on figure 7, and is the same for each beam. However, the velocity represented by the yellow arrow is seen differently by each beam. The first beam shows a projection toward the instrument, whereas the second projection on the second beam goes away from the ADCP. This is why ADCPs have several beams. By drawing lines perpendicular to the extremity of the two vectors, it is possible to get the velocity and the direction of the particles (figure 7(c)).

2.1.2 Advantages and limitations

ADCP offers several advantages in marine and freshwater research. One benefit is its ability to measure current speed at multiple depths simultaneously, allowing continuous and detailed profiling of currents throughout the water column. ADCPs mounted on ships or underwater vehicles can quickly cover large areas, giving a quick comprehension of currents in a large zone. The use of the Doppler effect enables ADCPs to measure water speed with high precision, and they are known for their reliability in various environmental conditions. ADCPs also conduct non-intrusive measurements using acoustic waves, ensuring that they do not interfere with the aquatic environment or damage underwater ecosystems or structures. These devices also offer three-dimensional data, delivering current information in all three dimensions (x, y, z), which is essential for detailed studies of ocean and river dynamics. They can be used in diverse environments, including rivers, estuaries, lakes, oceans.

However, ADCPs come with some limitations. They are expensive instruments to purchase and maintain, which can be prohibitive for some projects or institutions. The data collected by an ADCP is often complex and requires advanced analysis and interpretation. ADCPs may also be sensitive to acoustic interference from other underwater sound sources, potentially affecting measurement accuracy or creating back-scattering at surface layer. There are many phenomena which could interfer with the current measurement at the surface, such as wave or wind noise, air bubbles formation, anthropogenic noises, or thermocline/halocline reach. The maximum depth at which an ADCP can profile is limited by the strength of its acoustic signal and water conditions, such as turbidity or salinity. Proper calibration is necessary to ensure accurate measurements, which may demand additional effort and time. Even if acoustic waves do not interfere with the aquatic environment, some marine organisms may still be affected. For example, the frequency range of clicks emitted by bottlenose dolphins (*Tursiops truncatus*) spans from 120 Hz to 300 kHz (Zhang et al., 2017). This range partially overlaps with the operating frequencies of certain long-range ADCPs, which emit signals between 100 kHz and 2000 kHz. The influence of *Tursiops truncatus* on ADCP performance was also analyzed in the same study (Zhang et al., 2017). The results indicated that when the click frequencies of dolphins coincide with the ADCP operating frequency, measurements of current velocity can be significantly compromised.

2.2 Studied sites

2.2.1 Selection of sites

Available sites were given by the Autorisation d'Occupation Temporaire (Temporary Occupation Permit) (AOT) (see table 1). Due to the limited availability of three ADCP devices, three specific sites were selected for deployment. The selected points are the points 1, 7 an 9, respectivelly "Pointe de la Revellata", "Baie de Calvi" and "Pointe de Caldanu" (figure 8). These sites were selected because they represent a large coverage of the bay. Two of them are located at the extremes of the bay, enabling measurement of fluxes entering from the southwest (site 1 - "Pointe de la Revellata") and northeast (site 9 - "Pointe de Caldanu"). The third site (site 7 - "Baie de Calvi") is centrally positioned, allowing the analysis and measurement of current trends in the heart of the bay.

Two fixing devices for the instruments are available depending on the sites. For sites located less than 10 meters from the seagrass bed (sites 2, 3 and 4), the current meter (or ADCP) is fixed using a removable device composed of two sand screws per current meter, in accordance with Order No. 123/2019 of June 2019 (de La Faverie du Ché, 2019), prohibiting any anchoring in seagrass beds. As we don't anchor any ADCP into the seagrass bed, we only use weighted block (see figure 9). The measurement points are located on the ocean floor at depths of 21 m, 31 m and 36 m.

Table 1: Site characteristics for ADCP deployment. The chosen sites are the site 1, 7 and 9 (MDS: Minimum Distance to Seagrass. WB: Weighted Block. SS: Sand Screw).

Site	Description	Equipment	Longitude	Latitude	MDS (m)	Depth (m)
1	Pointe de la Revellata	WB	8.730858	42.584669	176	36
2	Sillon (Alga)	SS	8.733539	42.570836	2.5	28.5
3	Herbiers (Alga)	SS	8.732104	42.570301	0	28
4	Tache de matte (Alga)	SS	8.731730	42.570892	10	27.5
5	Baie de Calvi (Saint-François)	WB	8.746469	42.572423	62	37.3
6	Baie de Calvi (Citadelle)	WB	8.762366	42.571578	18	32
7	Baie de Calvi	WB	8.779025	42.565393	18	21
8	Baie de Calvi	WB	8.796245	42.596601	111	34.5
9	Pointe de Caldanu	WB	8.791392	42.585137	105	32

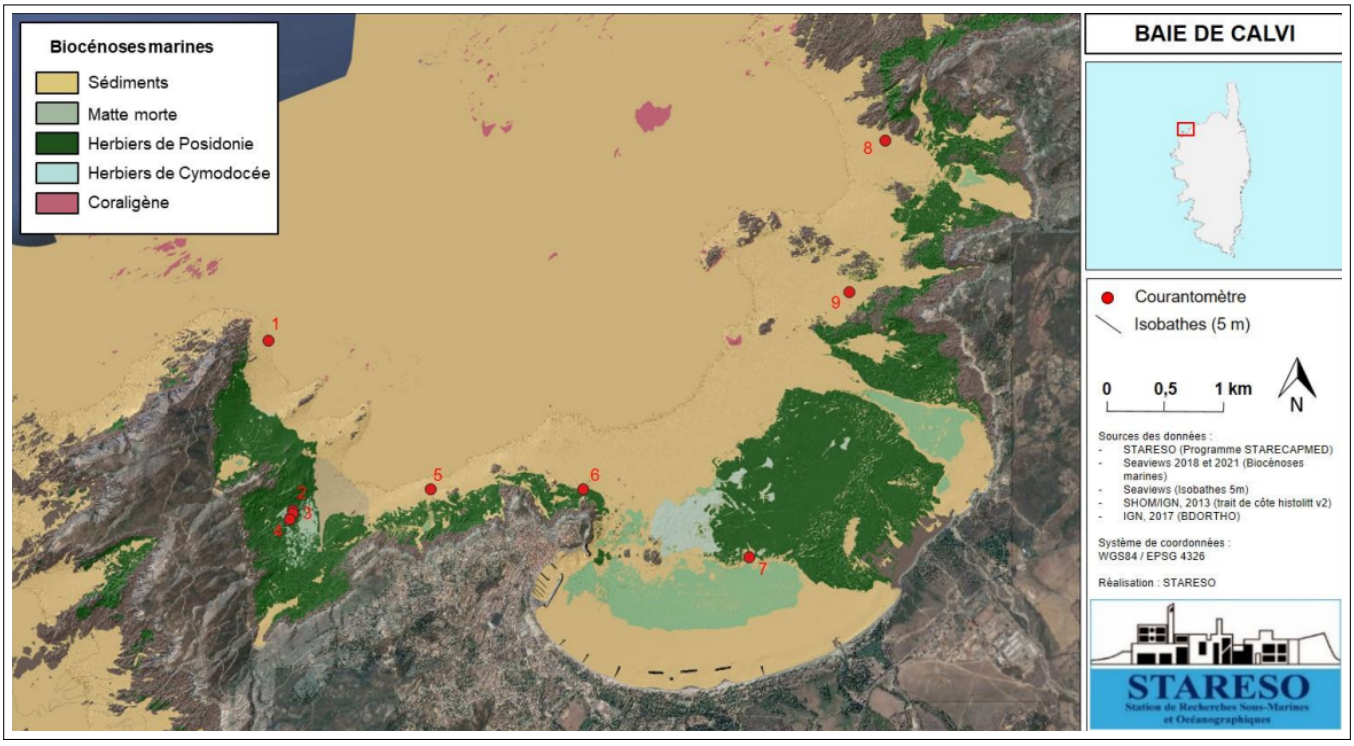

Figure 8: Sites identified for the deployment of the ADCPs. Description of the different sites is given in table 1.

2.2.2 Measurement period and duration

Each measurement is planned over a period of one month. The sampling periods are detailed further in this report. However, given that the battery life is estimated to be between 20 and 30 days, this timeline may need to be adjusted accordingly. Currents data are recorded every 20 minutes. Temperature and conductivity sensors are deactivated to ensure a better autonomy to the instrument.

2.2.3 Description of Seaguard II ADCP

The ADCPs used for the campaign are Seaguard II from the company Aanderaa (a picture of the instrument on figure 4). The current meter has a total height of 60 cm with a diameter of 13 cm. Two parts can be described separatly. The "body" where all the electronics resides is the Seaguard II platform. The "head" is the sensor measuring the currents: the Doppler Current Profiler Sensor (DCPS). Other sensors are installed on the platform, such as a temperature sensor, a conductivity sensor or an oximeter. However, they are deactivated to allow greater autonomy.

To configure the ADCPs, we use a computer connected to the instrument via USB and the software provided by the manufacturer Aanderaa. This specialized software allows to adjust the parameters of the ADCP. Through this interface, it is possible to adjust the parameters for each situation.

2.2.4 ADCP configuration

Table 2: Technical specifications of the measuring points.

Site	Description	Depth (m)	Number of Cells
Site 1	Baie de Calvi (Pointe de la Revellata)	36	75
Site 7	Baie de Calvi	21	30
Site 9	Baie de Calvi (Pointe de Caldanu)	31	65

For our measurements, we favor a high frequency of 600 kHz. This allows to collect more samples over a given distance, although the range is reduced. Given the shallow depths of our sites (21, 31 and 36 meters), this approach allows us to obtain a better resolution. Moreover, this frequency minimizes overlap with dolphin vocalizations.

One parameter to set is the number of cells. A cell refers to a specific depth layer or segment of water that the ADCP measures. As we saw previously, ADCPs use acoustic signals to measure the velocity of water at different depths, and these measurements are divided into discrete segments or "cells." Each cell represents a specific depth range, and the ADCP calculates the average current velocity within that range over a given period. Setting smaller cells offer an increased spatial precision, but increase the variance of the measured velocities. The variance is a measure of how much the values in a set of data differ from the mean of that set. In other words, it shows how dispersed the data are around the mean value (Nortek, 2021). The larger the variance, the more spread out the values are. Scattered data may include extreme or outlier values, increasing the risk of errors and reducing accuracy of the data. To reduce this variance, we space the frequency of measurements (or pings), which decreases the temporal resolution.

It is necessary to find a balance between spatial, temporal resolution and the variance. We set each cell to 1 meter high with an overlap of 50 cm. We deduct 1 meter from the bottom for the weighted block, the instrument and the "dead zone" between the sensor and the start of the measurements, as well as 5 meters from the surface to avoid back-scattering.

2.3 Deployment and retrieval procedures

The deployment of the ADCP is carried out using a boat, 2 divers and 2 other crew members on the boat. Once the boat reaches the site coordinates, the divers enter the water and accompany the descent of the instrument. The instrument is secured by a rope, held by the team remaining on the boat. It is weighted with a concrete base, into which a PVC pipe is inserted to hold the instrument in place (figure 9(a)). This method prevents the instrument from falling during measurements and keeps its head oriented towards the surface. A piece of neoprene is added around the instrument to stabilize it, even though a pitch corrector is included in the instrument software. A GPS point is recorded at the instrument's installation site to ensure it can be easily located during retrieval. The system will not be equipped with chains or surface buoys. Surface buoys are undesirable, as they can interfere with current measurements relying on acoustic signals. Thus, the deployment sites are georeferenced and located at relatively shallow depths. Instruments are therefore easy to locate. This setup also reduces the risk of boat incidents caused by other users encountering the buoys.

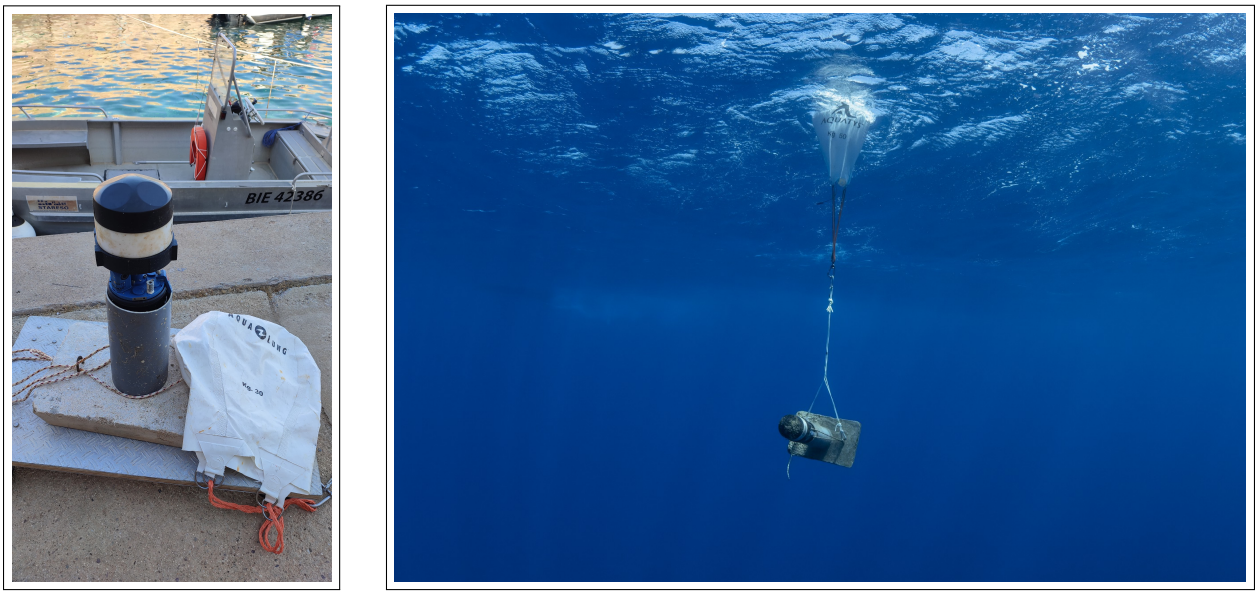

(a) (b)

Figure 9: (a) Picture illustrating the boat used to reach the site's coordinates. An ADCP, placed in its PVC pipe, weighted with a concrete base. A parachute, used to retrieve the instrument. (b) Illustration of an ADCP resurfacing under a parachute at the end of the campaign.

For the retrieval, divers return to the recorded GPS coordinates to attach a parachute to the ADCP (figure 9 (b)), allowing it to rise to the surface, where it is recovered by the team on the boat.

One objective is to optimize data collection by deploying the ADCPs as much as possible. However, launches were delayed due to bad weather conditions and hardware issues, including limitations related to the autonomy of the devices and the impossibility of recharging the batteries. Figure 10 illustrates the deployment periods. Only site 1 (Calvi Bay, Pointe de la Revellata) benefited from a good temporal coverage. In contrast, sites 7 and 9 (Calvi Bay and Calvi Bay, Pointe de Caldanu, respectively) could only be sampled once each. Thus, the ADCP at site 9 experienced a malfunction, resulting in almost no data being recorded.

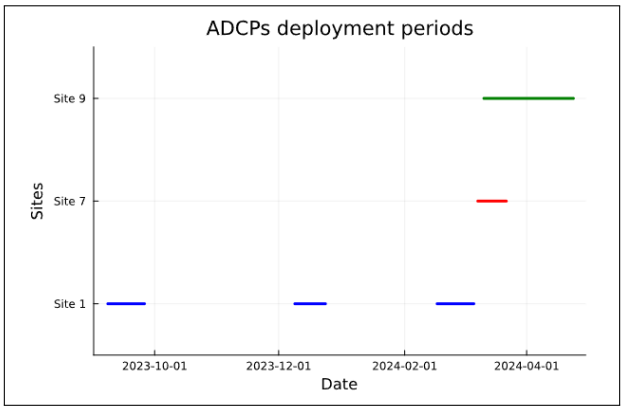

Figure 10: Deployment periods of the ADCPs, illustrating the frequency of deployments at various sampling sites.

2.4 Data collection and processing

2.4.1 Raw data collection

During the measurement period, the data is logged and stored on an SD card. When the instrument is retrieved, the data is transferred via a USB connection to a computer, using a software only compatible with Windows XP. The instrument generates files with a .data extension.

2.4.2 Software used for data processing

The .data files are processed using Data Studio 3D software, which extracts the data, gives the possibility to create profiles, and converts the results into CSV format. These CSV files are then further processed and analyzed using Julia or R. While the data appears accurate within the manufacturer's software, the software has issues when exporting CSV files, leading to many errors or duplicated information in the exported files.

2.5 Other data sources

2.5.1 Historical data

Previous measurements were conducted from 1998 to 2002, with an additional campaign from 2015 to 2018. A significant part of this study was to retrieve, extract, and process historical data to facilitate comparisons with each other and with the measurements conducted in 2023 and 2024.

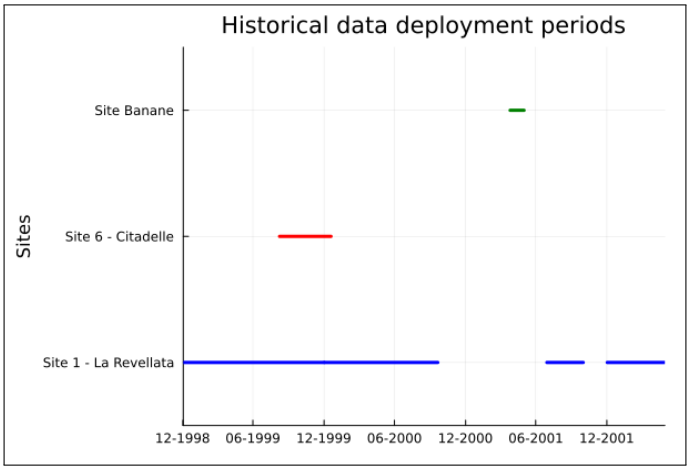

Figure 11: Deployment periods corresponding to the historical data from 1998 to 2002, illustrating the frequency of deployments at different sampling sites.

The historical data from 1998 to 2002 are primarily focused on a single site, "La Revellata", which has been studied much more extensively compared to the other sites (see figure 11). "Citadelle" is included into the AOT (figure 8), but "Banane" is not. This site is situated near the STARESO (yellow dot on figure 12). Rotor Current Meter (RCM) instruments have been used to estimate current speed and direction, equipped with a propeller to detect water velocity and a vane to determine the direction of the flow. These measurements provide a good estimate of the currents, capturing both the intensity and the orientation of the water movement.

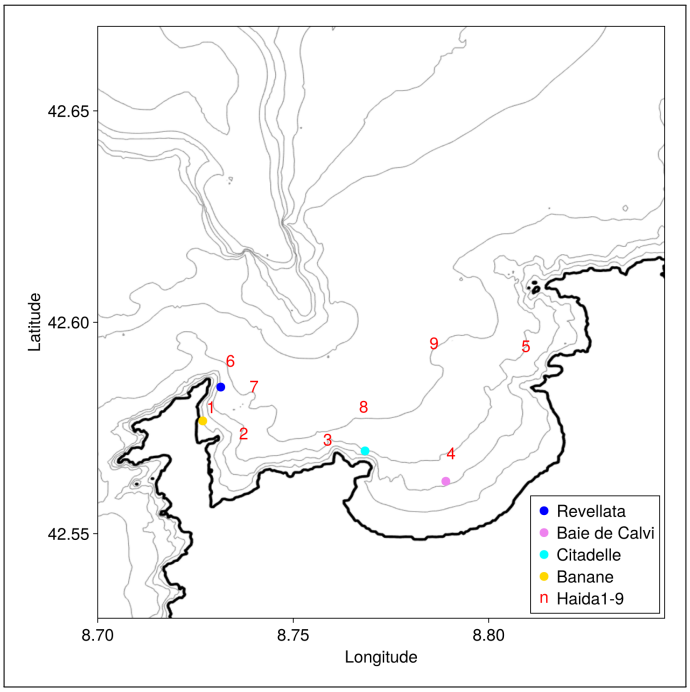

Figure 12: Map of the bay of Calvi, representing all the sites where data were collected during this study.

The campaign from 2015 to 2018 focused on sites other than the AOT. These campaigns covered 9 sites (see figure 12). Data from 2016 to 2018 were collected, as the results from 2015 did not specify which sites were studied. The depths of the Haida sites are now available: Haida sites 1 to 5 are located at 30 meters depth, while Haida sites 6 to 9 are at 60 meters depth.These data were collected using an RCM, which differs from an ADCP in that it measures currents at a single, fixed depth rather than providing a vertical profile of the water column. Below is a list of the days covered by the measurement campaign across all the sites:

- 2016 : 09/08 - 12/09 - 16/10 - 16/11 - 22/11 - 13/12
- 2017 : 20/02 - 12/04 - 30/05 - 15/06 - 04/08 - 20/09 - 09/11
- 2018 : 09/01 - 16/02 - 17/04 - 17/05 - 5/07

2.5.2 Model data

CORSE400, the hydrodynamic model MARS3D for the CORSE region (MARC_L2-CORSE400) is a 3D model with a spatial resolution of 400 meters across 30 levels. It provides data on currents, sea levels, temperature, and salinity every 3 hours.

2.5.3 Meteorological data

Meteorological data are available for the period of immersion of the devices and for historical data. These atmospheric data were measured by a meteorological station located at the western end of the Bay of Calvi, at the level of "Punta de la Revellata". These data are correlated with the hydrodynamic measurements to estimate whether or not the winds affect the currents.

2.6 Data analysis methodology

The primary goal of this study is to identify trends and anomalies in the currents of Calvi Bay, in order to determine spatial or temporal variabilities. Initially, the analysis assesses whether wind has a significant impact on the currents. As highlighted in the introduction, atmospheric conditions strongly influence the hydrodynamics of the LPB (Astraldi et al., 1994). In Corsica, strong winds, particularly during specific periods (Poulain et al., 2012), are expected to have a pronounced impact on hydrodynamics, especially in shallow areas. Profiles of current velocities across the entire water column are created to examine tendencies in current speed and direction during 2023 and 2024 measurements. These profiles illustrate the u and v components of current velocity.

To better identify trends and anomalies in these data, the analysis is further refined by incorporating mean velocity and standard deviation profiles. To enhance interpretation, figures are plotted for specific depths: 5, 15, 25, and 35 meters at site 1 - "Pointe de la Revellata," and 5, 10, 15, and 20 meters at site 7 - "Baie de Calvi." Represented as vector time series, these figures are analyzed along with wind data from the same period to evaluate the correlation between currents and wind. Pearson's complex correlation is also applied to obtain quantitative results on whether or not a correlation exists between wind and currents.

For phenomena other than winds impacting currents, a rotary spectrum analysis is performed, in order to decompose the u an v component, allowing for an identification of cyclic patterns in the current dynamics.

In order to observe and understand the evolution of currents over several campaigns, this study generates plots of current speed and direction spanning the period from 1998 to 2002. These visualizations are completed by the inclusion of maps that illustrate the principal dynamics governing the currents within Calvi Bay. To ensure the reliability and accuracy of these maps, the CORSE400 model is employed as a verification tool.

2.7 Expected results

The expected results of this study rely on the interaction between environmental and oceanographic factors impacting the hydrodynamics of the Calvi Bay. The strong winds in Corsica, particularly during specific periods (Poulain et al., 2012), have a strong impact on hydrodynamics, especially in shallow areas. The bay hydrodynamics could be influenced by the WCC, which flows along the western coast (Ahumada and Cruzado, 2007). We anticipate detecting this current within the bay, especially on the site 1 - 'Pointe de la Revellata", as a flow moving from the southwest towards the northeast.

The presence of an underwater canyon, situated approximately 3 kilometers off the Corsican coast may exerce an influence on the water dynamics within the bay, particularly during storm events (Skliris et al., 2001).

Norro (1995) detected gyres that can influence the currents' speed and direction within the bay. The role of the Coriolis force in gyre formation and behavior is well known, as it deflects currents. However, we may not have studied enough sites to confirm the presence of a gyre in the bay. Nevertheless, the maps and the model used for verification in this study could provide evidence on the existence of gyres in the area.

3 Results & analysis

3.1 Presentation & interpretation of the results

This section presents the results obtained during the sampling campaign conducted at sites 1 and 7, specifically “Pointe de la Revellata” and “Baie de Calvi”, and will give at the same time interpretations of these findings.

3.1.1 Field site 1: “Pointe de la Revellata”

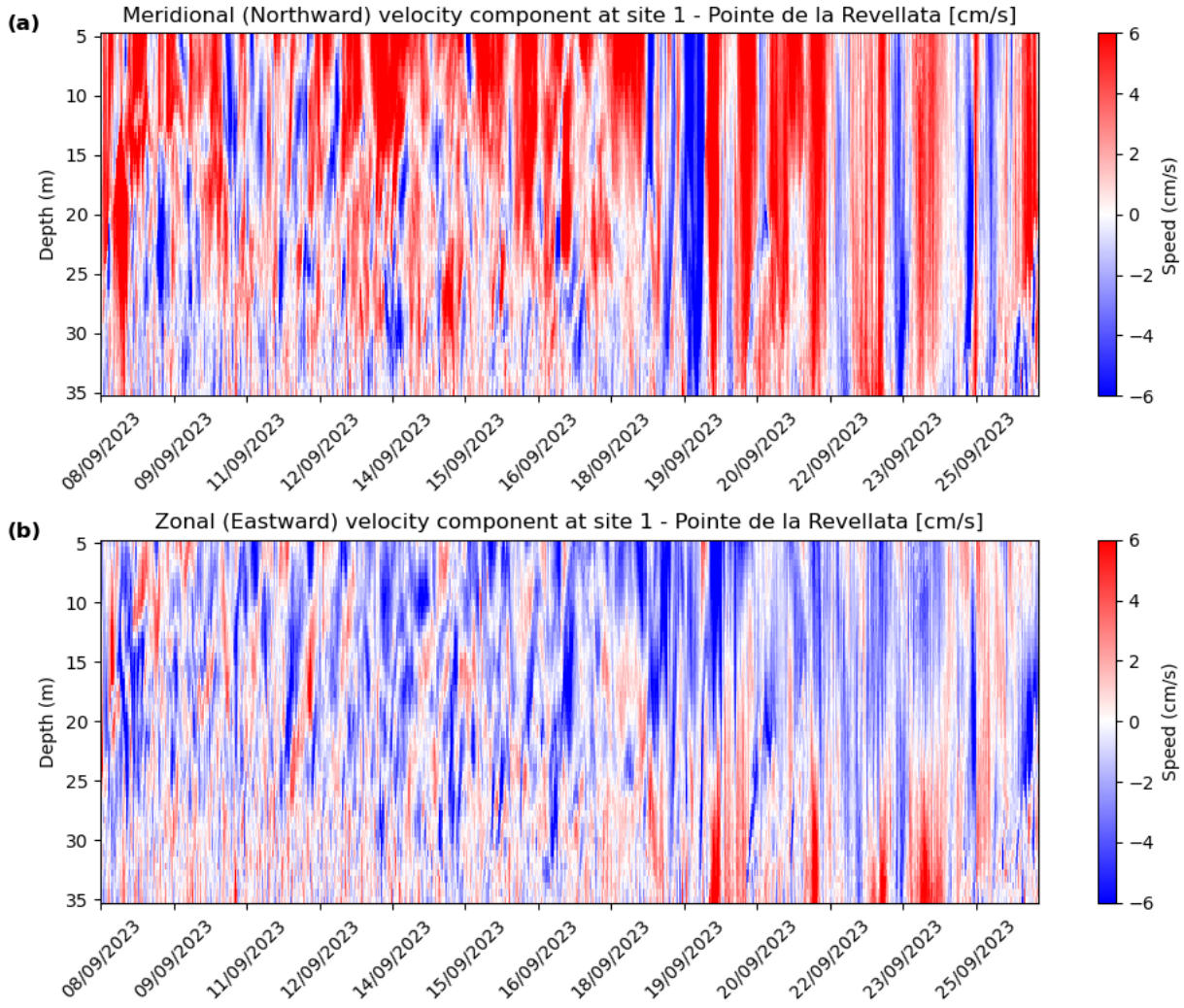

Figure 13: Northward (a) and eastward (b) velocity component in cm/s, at the site 1 - “Pointe de la Revellata”, from the 8th of September to the 26th of September 2023. Negative values represent currents flowing opposite to the cardinal point.

Figures 13, 17, 20 and 23 display profiles with time on the x-axis and depth on the y-axis. Negative values represent currents moving in the opposite direction to the indicated cardinal point: positive values indicate a northward (a) or eastward (b) current, while negative values represent southward or westward currents. Values shallower than 5 meters are not taken into account, as the values are affected by artefacts coming from the back-scattering surface.

Figures 14, 18 and 21 represent time series of speed and direction currents for the site 1 - “Pointe de la Revellata”. Several depths were extracted : 5, 15, 25 and 35m. The magnitude and direction of the currents are computed, giving vectors for each measurement. A vector with a large amplitude, represented by an arrow with a tip far from its origin, indicates a strong current. The graphs are designed so that the arrows point in the direction corresponding to the cardinal points. For example, an arrow pointing upwards indicates a current flowing northward. Wind speed and direction data are also provided. To facilitate an easy comparison of current behavior with wind patterns, we do not focus on the wind’s origin, but rather on the direction in which the wind is heading.

September 8th to September 26th of 2023

For the figure 13 representing the site 1 - “Pointe de la Revellata” from September 8th to September 26th of 2023, higher velocities are observed near the surface, between 6 and 9 cm/s. The northward component generally dominates the southward, while the westward component prevails over the eastward, with velocities from -4 to 2 cm/s. We observe from September 19th to September 20th an inversion of the northward velocity component. During this period, the direction of the current is heading south for this component. While the pattern for the east-west component is less pronounced on this day, it remains detectable, with a westward velocity of approximately 4 cm/s.

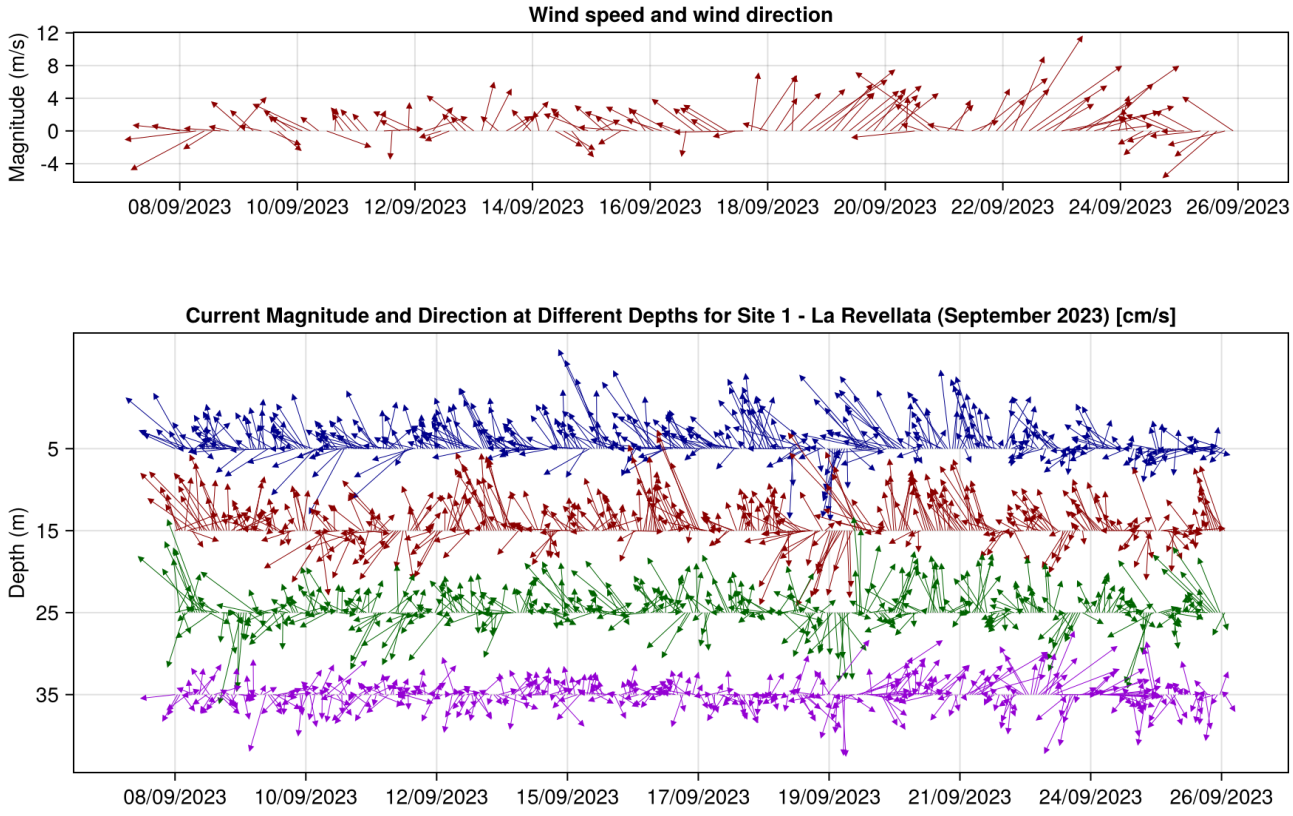

Figure 14: Current magnitude and direction at different depths, at the site “Pointe de la Revellata”, from September 8th to September 26th 2023. The size of the arrows express the speed of the current, maximum being 13 cm/s. The graph has been drawn, so the direction of the arrows reflect the cardinal points.

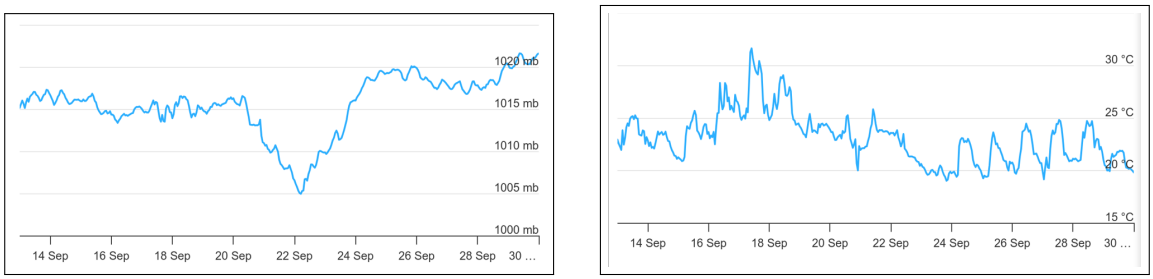

(a) (b)

Figure 15: Atmospherical pressure (a) & air temperature (b) in Punta de la Revellata weather station for the second half of September 2023.

Like in the profile illustrated by figure 13, we observe a dominance of the north speed in figure 14. The inversion from September 19th to September 20th is also noted. At depths of 15 and 25 meters, the patterns are similar, with currents at 5 meters predominantly heading north. Whereas at 35 meters, the currents are more variable with a lower magnitude, but align with the trends at other depths during the anomaly of September the 19h. The 35 m depth might be subject to a thermocline, as thermoclines typically form during the summer between 25 and 30 m, and can persist into October (Remy, 2016).

When examining the wind direction and intensity for the month of September in figure 14, we observe generally low wind intensities with a magnitude of 4 m/s. The end of the month shows higher wind magnitudes, with a noticeable dominance of northwest or northeast winds. However, September 19th appears to be a pivotal date. Before this day, the winds primarily head northwest. Afterward, they continue to head northeast but with increased intensity. Both the wind direction and intensity decrease on September 25th. The current inversion observed in figure 13 occurred on the same day as this shift in wind direction, suggesting a possible connection between these two events.

A meteorological front could be responsible of this change of velocity and direction in both currents and winds. Before the passage of a meteorological front, the temperatures increase, the pressure falls and the wind speed increases. Once the front is upon a location, the temperatures increase even more, the winds change direction, and the pressure stops falling (Gregorius and Blewitt, 1998). The strongest winds are not usually expected at the edge of a low-pressure system, as their intensity is typically higher close to the system's center. Nevertheless, localized factors can influence wind strength at the edges. A delay between changes in wind and pressure is indeed to be expected. This lag can result from the dynamics of atmospheric circulation and the response time of the local environment to broader meteorological changes. Looking at the meteorological data from the Punta de la Revellata weather station (figure 15), we observe a significant pressure drop on September 22nd. Prior to this, the temperature rose on September 18th and then subsequently decreased.

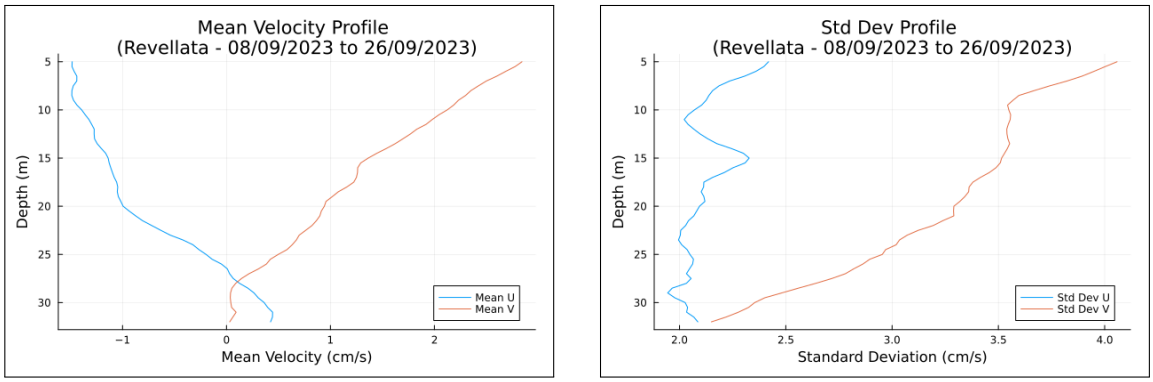

(a) **(b)**

Figure 16: Mean velocity (a) and standard deviation (b) profiles at "Pointe de la Revellata" (08/09/2023 to 26/09/2023).

Figure 16 presents the profiles of mean velocity and standard deviation for the u and v components measured at "Pointe de la Revellata" between September 8 and 26, 2023. As expected for this site, the values of both velocity components are higher near the surface, reflecting the influence of winds and surface marine currents. At greater depths, velocities gradually decrease due to friction within the water column. Regarding the standard deviation, greater variability is observed near the surface, indicating the impact of dynamic processes such as wind fluctuations. In contrast, the standard deviation decreases with depth, signaling more stable hydrodynamic conditions. These results align with the expected dynamics for this site and with the velocity shown on figure 13 and 14, with strong variability in surface layers and increasing stability at greater depths. As also observed in figure 13, the currents are oriented toward the northwest.

December 9th to December 24th of 2023

The water column data shown on figures 17 and 18 are derived from measurements taken at site 1 - "Pointe de la Revellata" from December 9th to 24th, 2023. The water column is less stratified than in September 2023 (figure 13), appearing more uniform compared to that previous month. This homogeneity is due to stronger winds, mixing the layers, and leading to a less pronounced thermocline (Remy, 2016).

This uniformity is more pronounced in the northward component than in the eastward component, potentially linked to the wind direction during December 2023. We observe eastward currents at depths of 35 to 25 meters with velocities of 10 cm/s occurring periodically over several days, but without a clear frequency. These events are also noticeable on figure 18. They can be observed at the same depths as in figure 17, on September 10th, 14th, and 21st. These occurrences are the most prominent.

The figure 18 shows that wind magnitudes are higher than in September 2023, particularly from December 10th to 17th and again from December 21st to 24th. The magnitude and the direction of the currents of the surface layer, represented in figure 18, follows the wind behaviour. This water layer appears to be influenced by the winds, while the deeper layers seem to be less affected by wind conditions.

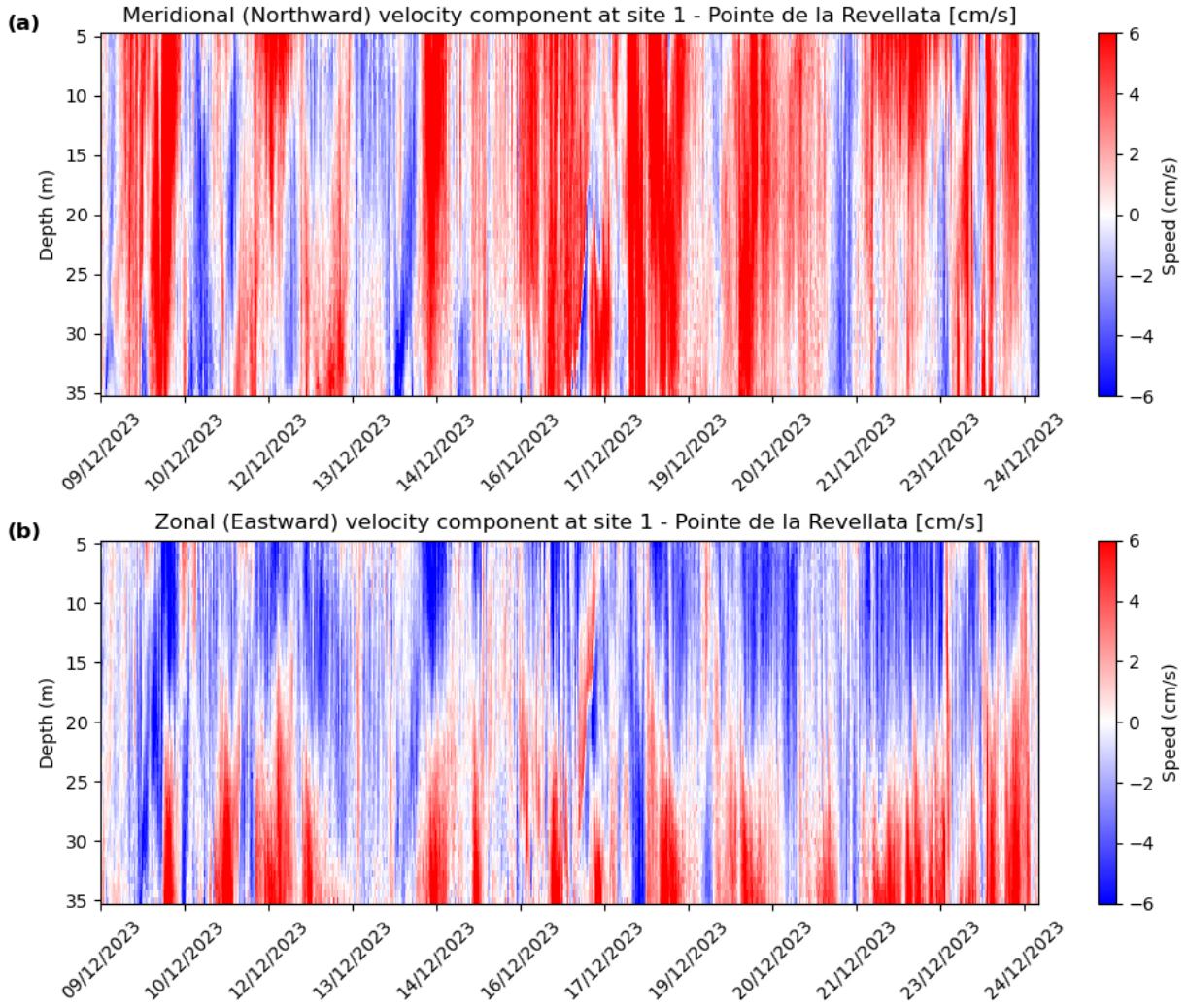

Figure 17: Northward (a) and eastward (b) velocity component in cm/sec, at the site 1 - "Pointe de la Revellata", from the 9th of December to the 24th of December 2023.

While the northward component of the currents aligns with the northeast-flowing wind, the eastward component, however, moves in the opposite direction. The northward component is particularly prominent at 5 meters depth in figure 18, with the exception of December 15th to 16th, when the northward velocities decrease. A similar trend is observed at depths of 15, 25, and 35 meters. The northward currents at these depths generally follow the same pattern, with a slight decrease in strength as depth increases. These variations suggest that the wind may influence the upper layers more significantly, while the deeper layers exhibit a less pronounced response. The consistency of the northward flow across different depths indicates a strong interaction between the wind and the surface waters, while the temporary decrease around December 15th to 16th could be related to changes in wind conditions or other factors affecting the flow.

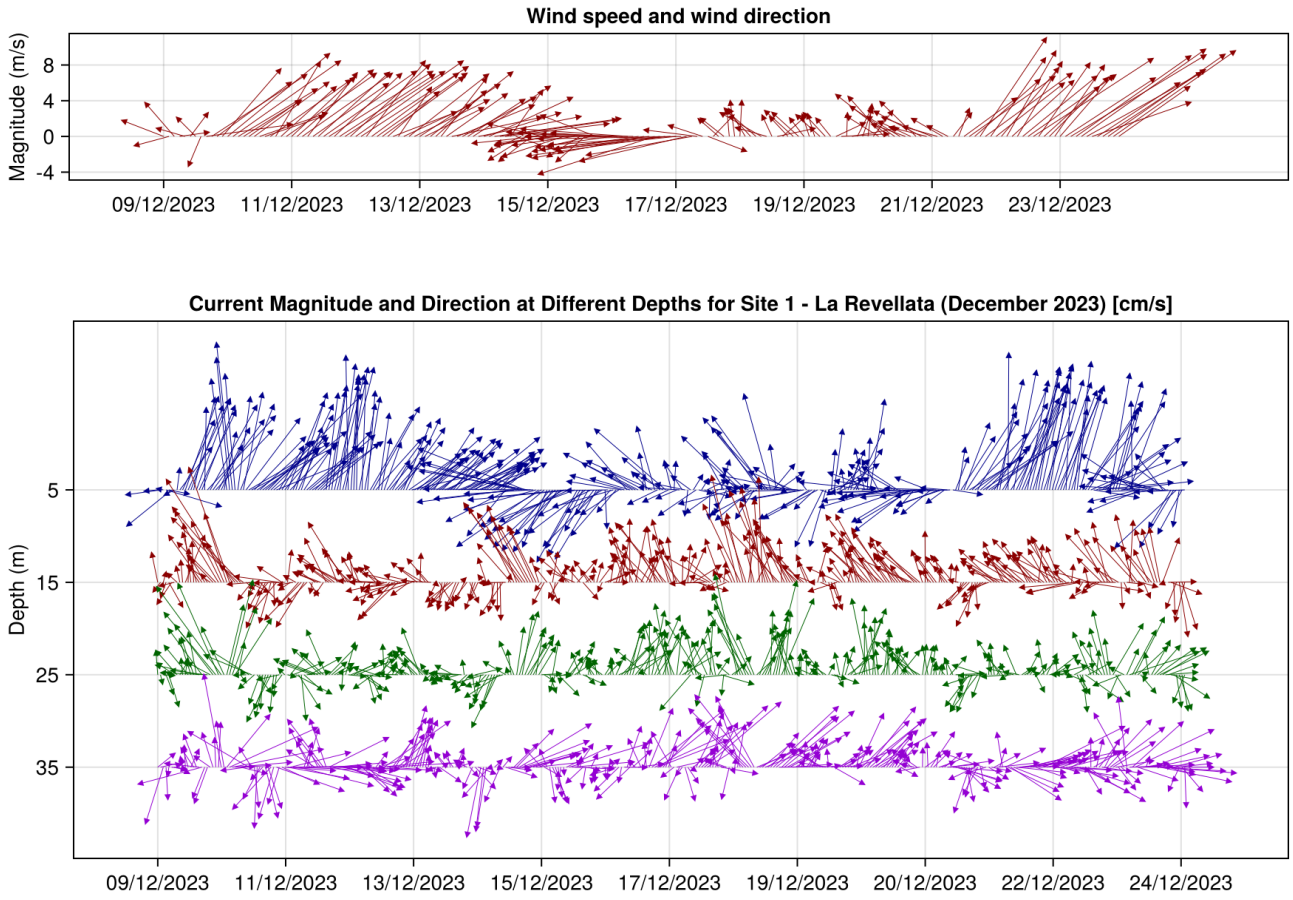

Figure 18: Current Magnitude and Direction at different depths, at the site "Pointe de la Revellata", from December 9th to December 24th 2023. The size of the arrows expresses the speed of the current, with a maximum of 17 cm/s. The graph has been drawn so the direction of the arrows reflects the cardinal points.

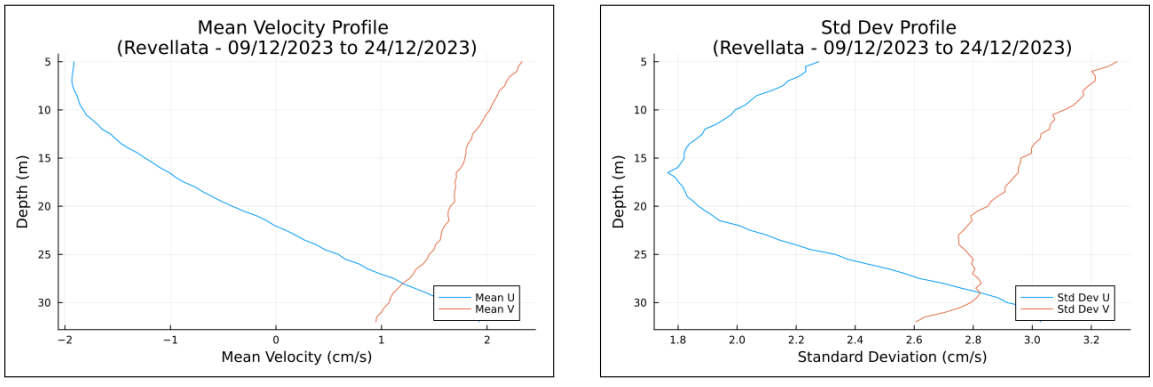

(a) **(b)**

Figure 19: Mean velocity (a) and standard deviation (b) profiles at "Pointe de la Revellata" (09/12/2023 to 24/12/2023).

The analysis of currents at different depths shows characteristic means and standard deviations for the *u* and *v* components (figure 19). Regarding the u component on the mean velocity profile (figure 19(a)), there is an inversion of currents between the surface and the bottom, with velocities ranging from -2 to 2 cm/s, indicating a change in direction between the shallow and deeper layers. For the *v* component, the currents are weaker at depth compared to the surface, where the velocities are higher (ranging from 2 to 1 cm/s). The variability of the currents is very high both at the surface and at depth (figure 19(b)). For the *u* component, variability is high at the surface (2.4 cm/s) and at a depth of 30 meters (3 cm/s), but remains low in the intermediate layers. Similarly, the *v* component shows very high variability at the surface (3.2 cm/s), which decreases but remains strong at depth (around 2.6 cm/s). These observations highlight a strong dynamic in the circulation, with unstable currents for the *u* component.

February 17th to March 6th, 2024

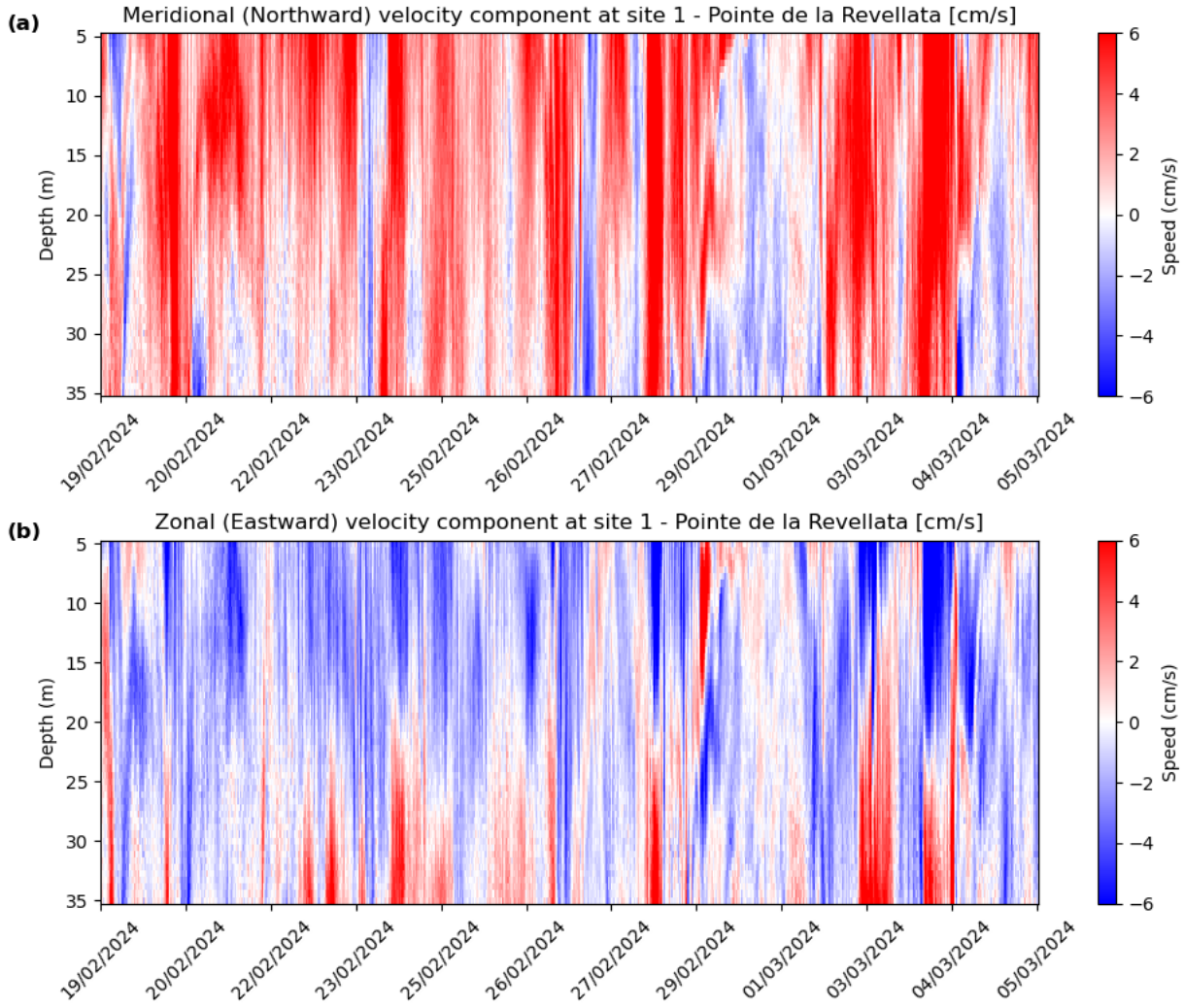

Figure 20: Northward (a) and eastward (b) velocity component in cm/sec, at the site 1 - "Pointe de la Revellata", from the 17th of February to the 6th of March 2024.

Between February 17th and March 6th, 2024 (figure 20), the water column shows a continued homogeneity in the *v* component of the currents, with a noticeable decrease in velocity early in March, potentially even indicating an inversion. In contrast, the *u* component exhibits more pronounced currents in March, with velocities ranging from -2 cm/s to -6 cm/s, suggesting a shift in current dynamics. These changes are reflected in the corresponding time series data (figure 21), which also highlight some periodic shifts in current direction at deeper levels. However, the wind conditions do not appear to align with these changes, raising questions about the exact driving forces behind the observed current patterns.

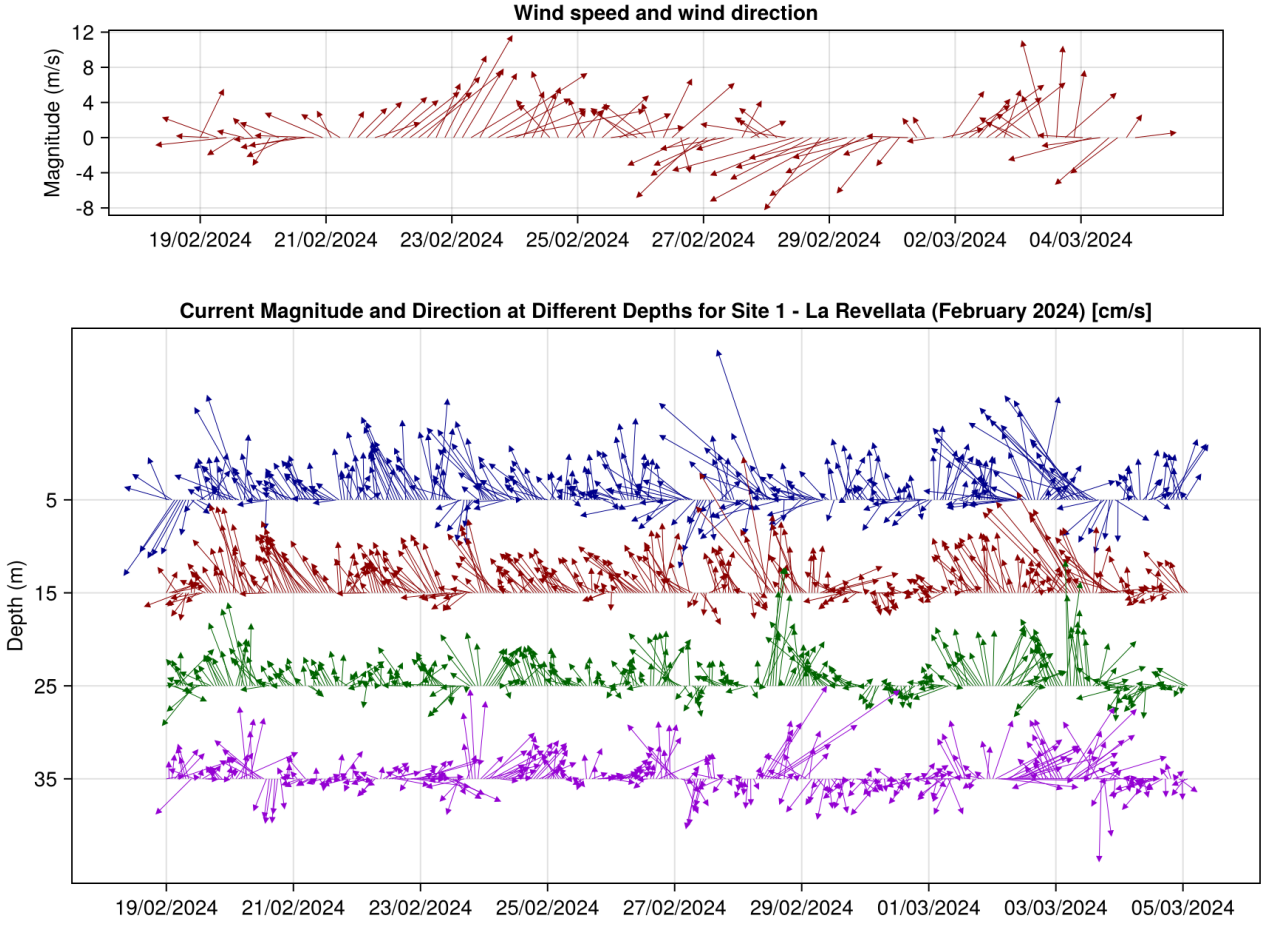

Figure 21: Current Magnitude and Direction at different depths, at the site "Pointe de la Revellata", from February 19th to March 5th 2024. The size of the arrows express the speed of the current, maximum being 16 cm/s. The graph has been drawn so the direction of the arrows reflect the cardinal points.

The mean current velocity profiles (figure 22(a)) reveal an inversion in the *u* component, with velocities shifting from -2 cm/s to 1 cm/s. This pattern remains stable up to about 10-15 meters, after which a gradual change occurs. For the *v* component, the velocity decreases from 3 cm/s to 1 cm/s, with a linear change observed from 5 to 35 meters. The standard deviation profiles (figure 22(b)) show a behavior similar to that observed for December 2023 (figure 19(b)). The *u* component demonstrates high variability at the surface (2.50 cm/s), likely influenced by wind conditions, while variability decreases at a depth of 20 meters (1.50 cm/s).

However, variability increases again towards the bottom (2.50 cm/s). The v component shows an instability across the entire water column, with slightly lower variability at depth (2.50 cm/s) compared to the surface (2.75 cm/s), suggesting a more uniform but still fluctuating current structure.

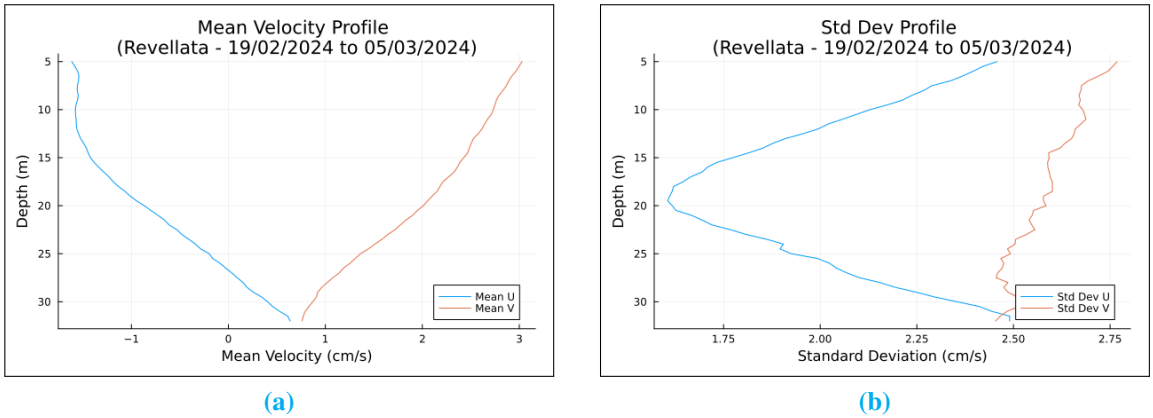

(a) (b)

Figure 22: Mean velocity (a) and standard deviation (b) profiles at "Pointe de la Revellata" (19/02/2024 to 05/03/2024).

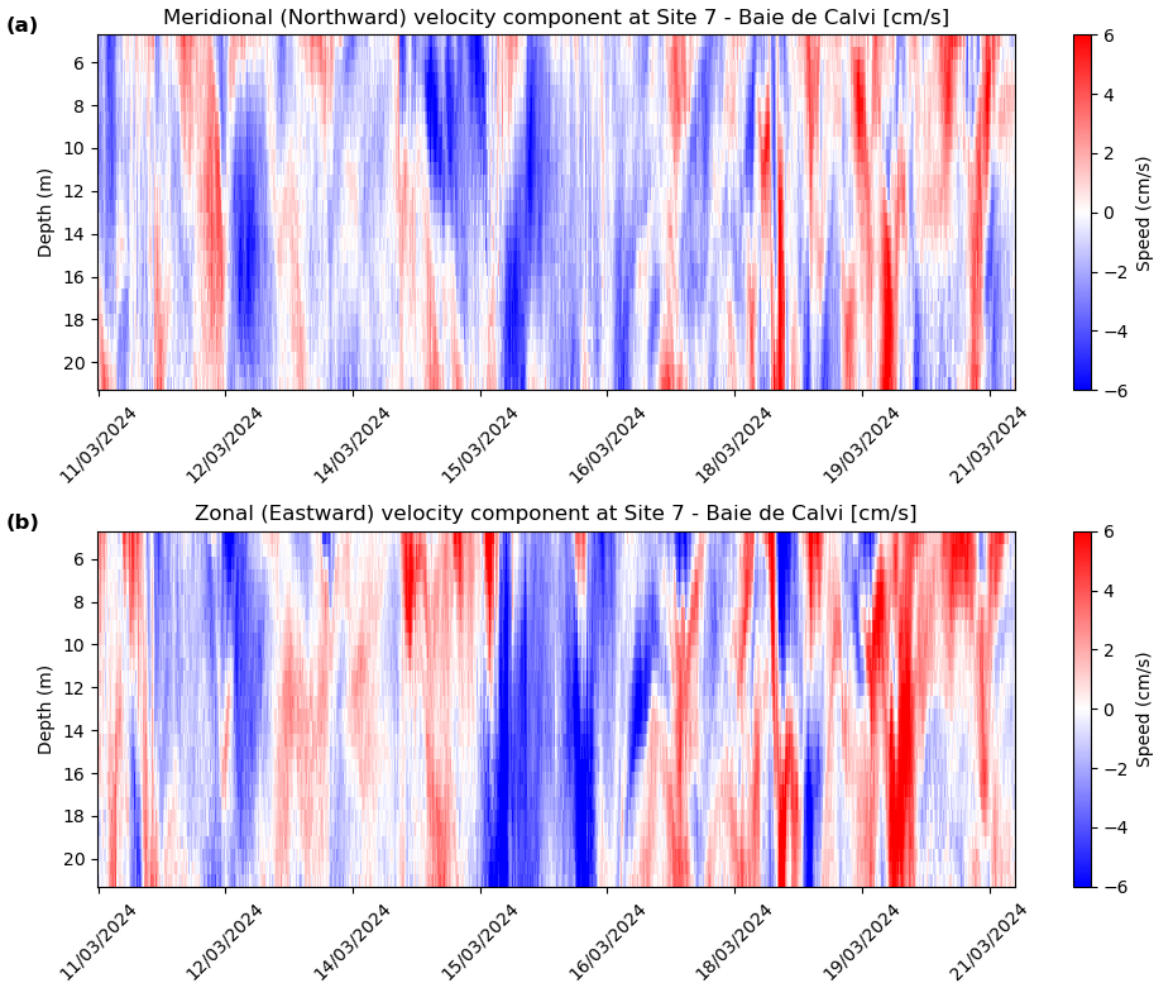

Figure 23: Northward and eastward velocity component in cm/sec, at the site 7 - "Baie de Calvi", from the 8th of March to the 22nd of March 2024.

3.1.2 Field site 7: “Baie de Calvi”

March 8th to March 22nd of 2024 :

From March 8th to March 22nd, 2024, the water column at this site reprsented on figure 23 shows a greater heterogeneity compared to site 1, “Pointe de la Revellata”. The currents are generally weaker and less pronounced, likely due to the location inside the bay, which is more sheltered from the stronger forces found further offshore. Notably, around March 16th, there is a significant current inversion, particularly in the u component, highlighting a shift in the direction of the currents. This inversion highlights the dynamic flow at this site, with more noticeable changes than at the outer location.

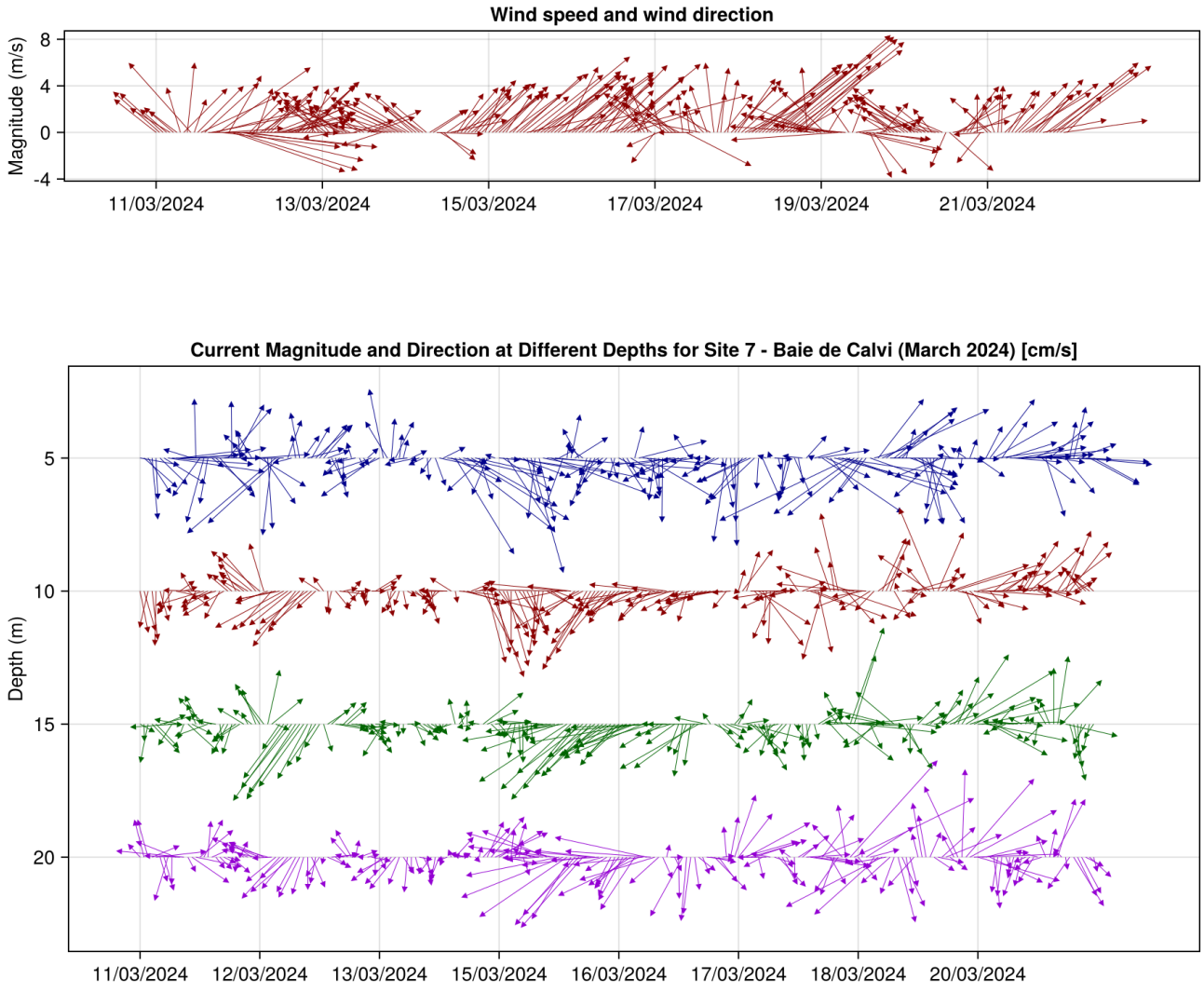

Figure 24: Current Magnitude and Direction at different depths, at the site “Baie de Calvi”, from March 11th to March 22nd 2024. The size of the arrows express the speed of the current, maximum being 11.8 cm/s. The graph has been drawn so the direction of the arrows reflect the cardinal points.

The time series (figure 24) reveal a significant disparity in the u component, with greater variability in the currents. In contrast, the v component is less pronounced, showing less unstable behavior. This trend is consistent throughout the entire water column, indicating that the northward currents are more variable, subject to fluctuations, while the eastward currents remain relatively steady across different depths. This further highlights the spatial and temporal variability in the flow at this site, with stronger shifts in the northward direction.

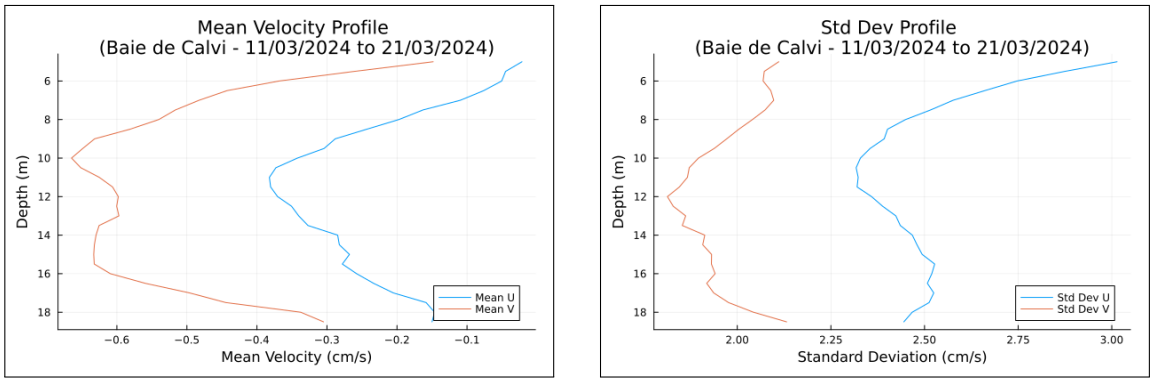

(a) (b)

Figure 25: Mean velocity (a) and standard deviation (b) profiles at "Pointe de la Revellata" (11/03/2024 to 21/03/2024).

The heterogeneity of the currents is also apparent in the profiles of mean velocity and standard deviation (figure 25). Compared to site 1, the currents at this location are less uniform, with significant variations in both velocity and variability throughout the water column. The mean velocity profiles indicate weaker currents in the bay, aligning with observations extracted from velocity component profiles (figure 23). Similarly, the standard deviation profiles reveal notable fluctuations, reflecting the less stable hydrodynamic conditions of this site. These findings emphasize the dynamic and variable nature of the currents in this location compared to the more exposed site 1 - "Pointe de la Revellata".

3.2 Identification of main factors influencing the currents

3.2.1 Correlation between winds and currents

To assess the correlation between wind direction and velocity with the currents' direction and velocity, we will use Pearson's complex correlation (Šverko et al., 2022). This method allows us to examine the relationship between the two variables, taking into account both their magnitudes and phases. By applying this technique, we can determine whether changes in wind conditions are closely linked to the observed variations in the currents, providing an understanding of the interactions between wind and currents.

The complex correlation r between the winds and currents can be calculated as:

$$r = \frac{\sum(x_i - \bar{x})(y_i^* - \bar{y^*})}{\sqrt{\sum(x_i - \bar{x})^2 \sum(y_i^* - \bar{y^*})^2}}$$

Where:

- x_i and y_i are the individual components of the wind and current vectors at each time point,
- $\bar{x}$ and $\bar{y}$ are the means of the wind and current components, respectively.

Amplitude of the result:

The absolute value of the result $|r|$ is between 0 and 1:

- $|r| \approx 1$: Strong correlation (winds and currents are aligned, in phase).
- $|r| \approx 0$: Weak or no correlation (no clear relationship between winds and currents).

The magnitude shows how closely the amplitude and direction of the two series (winds and currents) are related.

Angle of the result:

The argument (or phase) of the result $\angle r$ is given by the complex argument, calculated using:

$$\angle r = \text{atan}(\text{im}(r), \text{re}(r))$$

This function calculates the angle of the correlation in the complex plane.

- If $\angle r = 0°$, it means that the winds and currents are aligned (same direction).
- If $\angle r = 90°$ or $\angle r = -90°$, the winds and currents are orthogonal (independent in their direction).
- If $\angle r = 180°$, it means that they are opposite (same line of action but in opposite directions).

The results for the Pearson complex correlation are based on current data measured at a depth of 5, 15, 25, and 35 meters and are summarized in Table 3.

The results for the period from September 8 to September 29, 2023, reveal a generally weak relationship between wind and currents at the "Pointe de la Revellata", with notable variations by depth. At 5 meters, the complex correlation is $-0.095 - 0.083i$, with a magnitude of 0.13, indicating a weak interaction between the two variables. As the magnitude is weak, there is no need to analyze the associated phase. At 15 meters, the relationship remains weak with a magnitude of 0.097.

Table 3: Table of complex correlation between wind and currents, for different days and depths in "Pointe de la Revellata".

Period	Depth (m)	Complex correlation	Magnitude	Argument (rad)	Argument (°)
08 to 29/09/2023	5	$-0.095-0.083i$	0.13	-2.42	-138.68
08 to 29/09/2023	15	$0.097-0.003i$	0.097	-0.03	-1.67
08 to 29/09/2023	25	$-0.0012-0.006i$	0.006	-1.78	-102.05
08 to 29/09/2023	35	$-0.040+0.049i$	0.063	2.27	129.87
09 to 24/12/2023	5	$-0.67+0.24i$	0.71	2.79	160.22
09 to 24/12/2023	15	$0.12-0.19i$	0.22	-1.02	-58.57
09 to 24/12/2023	25	$0.16-0.18i$	0.25	-0.84	-48.21
09 to 24/12/2023	35	$-0.006-0.099i$	0.0995	-1.63	-93.65
19/02 to 05/03/2024	5	$-0.29-0.05i$	0.30	-2.97	-170.34
19/02 to 05/03/2024	15	$0.09-0.13i$	0.16	-0.97	55.94
19/02 to 05/03/2024	25	$0.20-0.23i$	0.30	-0.83	-47.87
19/02 to 05/03/2024	35	$0.12-0.09i$	0.15	-0.63	-35.96

At 25 meters, the correlation is almost negligible with a magnitude of 0.006. We could suppose that the currents at this depth are less influenced by the wind. However, at a depth of 35 meters, the magnitude is significantly higher than at 25 meters (0.063 vs 0.006). These results appear inconsistent. Specifically, the data at 35 meters are more strongly influenced by wind than those at 25 meters. Since the equation used is derived from Šverko et al. (2022), it is likely that the issue lies within the data itself.

During the period from December 9 to December 24, 2023, the relationship between wind and current becomes more pronounced, especially at 5 meters. The complex correlation is $-0.67+0.24i$, with a magnitude of 0.71, indicating a moderately strong interaction between the two variables. The argument of 160.22° suggests a significant phase shift, indicating a more complex dynamic in the interaction between the currents and the wind. At 15 meters, the correlation weakens, with a magnitude of 0.22 and at 25 meters, the correlation remains moderate with a magnitude of 0.25. Finally, at 35 meters, the correlation weakens further, with a magnitude of 0.0995, suggesting that other factors have a more significant impact on the currents at this depth.

For the period from February 19 to March 5, 2024, the relationship between wind and current remains relatively weak overall. At 5 meters, the complex correlation is $-0.29-0.05i$, with a magnitude of 0.30, suggesting that the wind plays a secondary role in driving the currents at this depth. At 15 meters, the magnitude of 0.16 indicate a more moderate interaction, and 25 meters, the relationship becomes slightly stronger, with a magnitude of 0.30, but it remains moderate compared to 5 meters. Finally, at 35 meters, although the correlation is weak with a magnitude of 0.15, there is still an interaction between the currents and the wind, but it is less significant than at shallower depths, suggesting influences from other marine forces.

Table 4: Table of complex correlation between wind and currents at different depths in "Baie de Calvi" (March 11th to 21st, 2024).

Period	Depth (m)	Complex correlation	Magnitude	Argument (rad)	Argument (°)
11/03 to 21/03/2024	5	$0.17 - 0.17i$	0.24	-2.36	-135.18
11/03 to 21/03/2024	10	$0.18 - 0.04i$	0.19	-0.22	-12.88
11/03 to 21/03/2024	15	$0.23 - 0.05i$	0.23	0.21	12.12
11/03 to 21/03/2024	20	$0.17 - 0.08i$	0.19	0.45	25.80

The results obtained between March 11 and March 21, 2024, in Calvi Bay show relatively weak correlations between wind and current dynamics. The magnitudes range from 0.19 to 0.24 across the various depths, indicating a moderate correlation between wind and currents at these depths. These values suggest that, while there is some influence of wind on the currents, the relationship is not as strong as expected. Poulain et al. (2012) have shown that winds have a strong impact on currents in shallow waters. The results suggest that the influence of wind on currents is present, but it is not dominant in Calvi Bay during this period. This site is well protected due to its location further into the bay, which likely minimizes the impact of wind on the currents.

The correlations obtained for both sites were very weak, whereas it was expected that the wind would have a significant influence both at the surface and throughout the entire water column. Further analysis of the current data is needed to understand what other factors might be influencing the currents.

3.2.2 Rotary spectrum analysis

In order to decompose the velocity components u and v and analyze the frequencies and recurring phenomena contributing to these vectors, the rotary spectrum method is applied (Gonella, 1972). This technique allows for the extraction of the amplitude and frequency of different components of the velocity vectors u and v. A straightforward way to represent a rotary vector in a plane is by using a complex variable.

For a two-dimensional velocity in the horizontal plane, such as wind or currents, the complex velocity is expressed as $w = u + iv$, where i denotes the imaginary unit. By applying the Fourier transform, the data are converted into the frequency domain, extracting the amplitude (in cm/s) and frequency (in cph : cycles per hour). Determining the frequencies at which these phenomena occur offer insights for identifying this phenomena.

The spectra show significant fluctuations, often due to noise or temporary phenomena. However, the general trend remains clear, with a rapid decay in amplitudes as a function of frequency. The highest amplitudes are located at low frequencies (between 0 and 0.2 cph), indicating that the currents are primarily dominated by slow, large-scale variations. For the measurements taken in September 2023 (figure 26 (a)), the values span frequencies from 0 to 0.2 cph. The magnitudes remain between 0.2 and 0.4 cm/s, indicating a relatively moderate influence of cyclical phenomena. We also observe an energy peak at 0.08 cph.

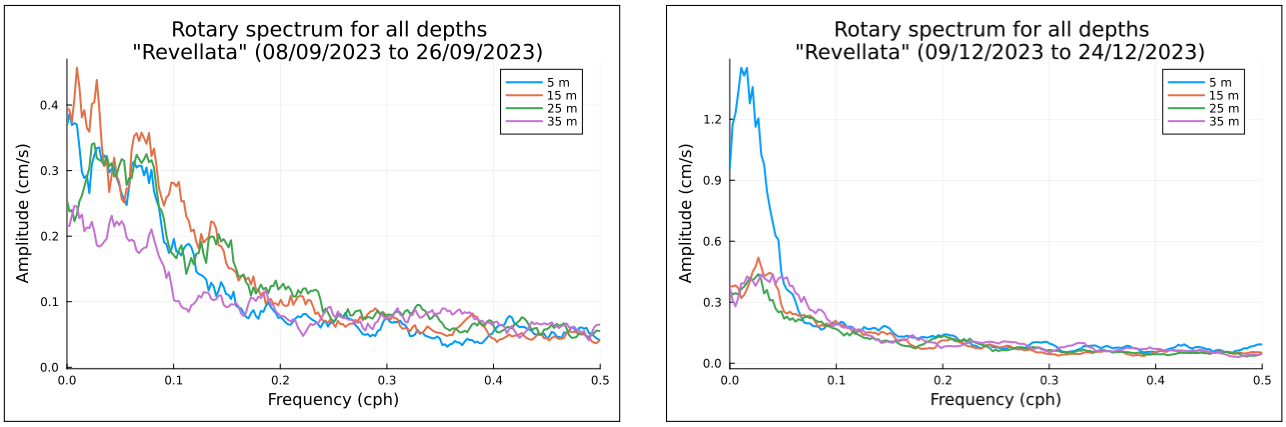

(a) (b)

Figure 26: Frequency decomposition using rotary spectrum analysis for data collected at the "Revellata" site, showing depths of 5, 15, 25, and 35 meters: (a) from September 8th to 26th, 2023, and (b) from December 9th to 24th, 2023. The x axis is in cycle per hour.

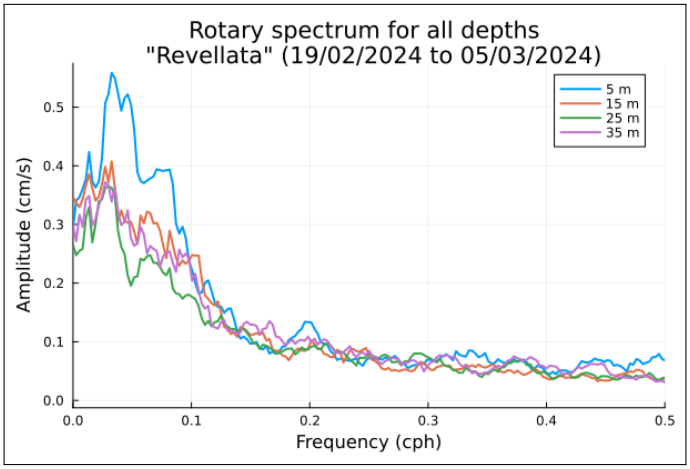

Figure 27: Frequency decomposition using rotary spectrum analysis for data collected at the "Revellata" site, showing depths of 5, 15, 25, and 35 meters, from February 19th to March 5th 2024. The x axis is in cycle per hour.

In December 2023 (figure 26 (b)), most depths show the same influence from cyclical phenomena (between 0.3 and 0.5 cm/s). However, the surface layer at 5 meters depth exhibits a strong amplitude of over 1.2 cm/s for a phenomenon occurring at approximately 0.03 cph.

In February 2024 (figure 27), a similar trend to December is observed. However, the phenomenon near the surface is weaker, with an amplitude of 0.5 cm/s compared to the 1.2 cm/s observed in December. This suggests a reduction in the intensity of surface-level phenomena during this period. We can observe a consistent trend across the data from all three periods, excluding the surface layer at a depth of 5 meters. As for 26, an energy peak can be observed at 0.08 cph.

For the period concerning the "Baie de Calvi" site (figure 28), in addition to showing the same trend as the " Pointe de la Revellata" site close to 0 - 0.1 cph, we also observe an energy peak at 0.08 cph. Tides in the Mediterranean, particularly at Calvi, follow a semi-diurnal cycle with a period of about 12 hours, or approximately 0.08 cycles per hour. This frequency is close to the one observed in our energy

spectrum, where a significant peak is found at 0.08 cph, with an amplitude of 0.4 cm/s. This could indicate a tidal influence, as tides typically generate currents with moderate amplitudes. In the Calvi area, the tidal amplitude can vary but generally remains in the range of 10 to 50 cm (Remy, 2016), which is consistent with the observed values. However, while this observation suggests a potential link to the tides, it is difficult to confirm this hypothesis definitively. Thus, the tidal currents in the the Ligurian Sea have a small contribution to hydrodynamics (Elliott, 1979). Therefore, although the connection between the energy peak and the tides is plausible, further studies and more detailed tidal data would be necessary to validate this hypothesis.

A strong energy in the low frequencies can be associated with tidal currents, internal waves, or large-scale oceanographic processes (Colling, 2001). The decrease in energy at higher frequencies can be attributed to energy dissipation. It is difficult to assign an energy peak to a specific phenomenon, as the energy is spread over a wide range of frequencies. Each frequency contributes only a small portion of the total energy, making it challenging to attribute an energy peak to a particular phenomenon.

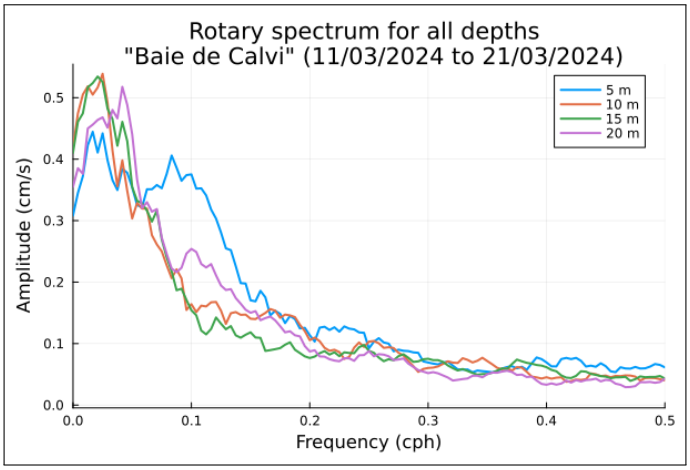

Figure 28: Frequency decomposition using rotary spectrum analysis for data collected at the "Baie de Calvi" site, showing depths of 5, 10, 15, and 25 meters, from March 11th to March 21st 2024. The x axis is in cycle per hour.

3.3 Temporal analysis of currents

3.3.1 Interannual comparison of currents

Figure 29 and Figure 30 present the temporal analysis of data collected at site 1, "Pointe de la Revellata," where high temporal resolution enables a detailed study. These graphs cover two distinct periods: 1998 to 2000, and 2001 to 2002.

Figure 29 depicts the variations in current speed, expressed in cm/s. These data reveal periods of more intense currents, and the moving average emphasizes slower, long-term changes in current intensity over the years. Figure 30 illustrates the temporal evolution of current direction, expressed in degrees. Significant variations can be observed across the periods, with pronounced oscillations that may reflect seasonal changes or specific events influencing the currents.

When comparing the two graphs, it is visible that changes in direction and speed are often correlated, suggesting a dynamic interaction between these two parameters. For instance, abrupt shifts in direction are sometimes accompanied by increases or decreases in speed. These observations may reflect local phenomena such as wind variations, tidal currents, marine fronts, or specific events impacting oceanic dynamics.

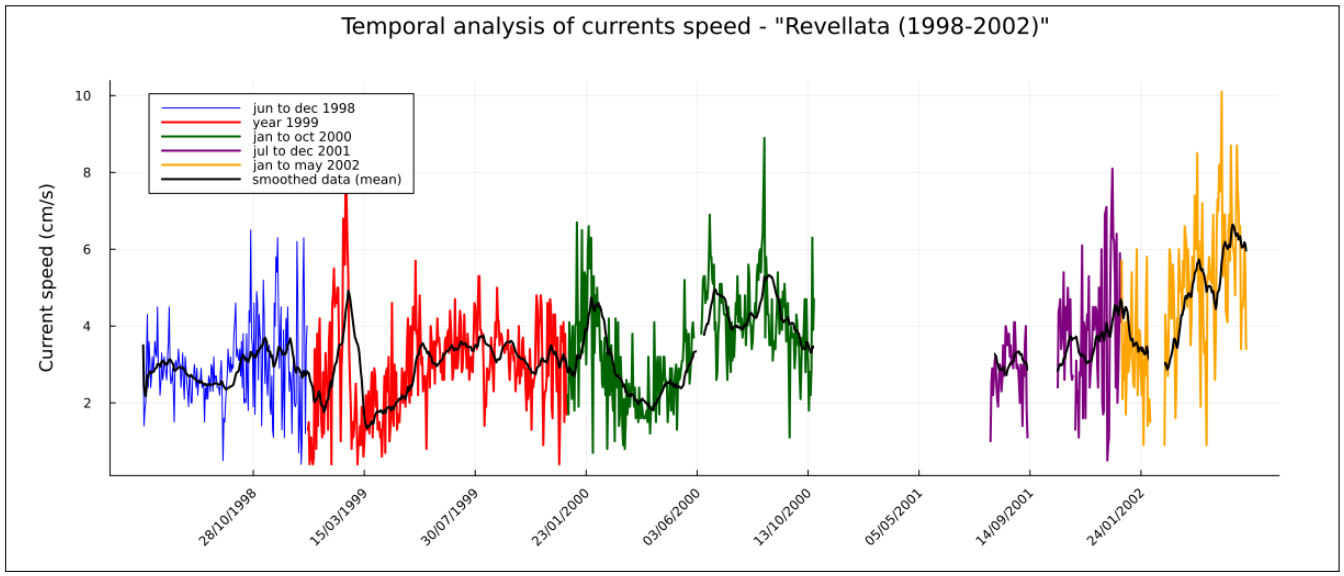

Figure 29: Temporal analysis of current speed at "Pointe de la Revellata" (1998-2002). The colored lines show the raw current speed data (in cm/s) for the same periods: June to December 1998 (blue), the year 1999 (red), January to October 2000 (green), July to December 2001 (purple), and January to May 2002 (orange). The black curve represents a moving average used to highlight the slow variations in current intensity over the years.

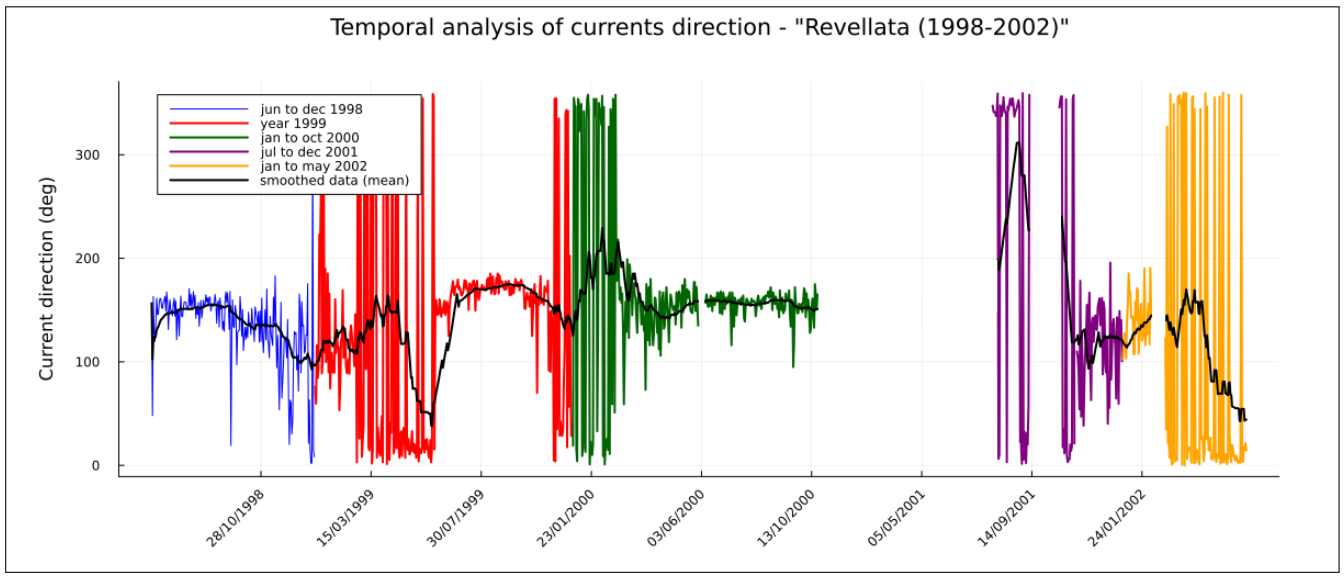

Figure 30: Temporal analysis of current direction at "Pointe de la Revellata" (1998-2002). The colored lines represent the raw current direction data (in degrees) for different periods: June to December 1998 (blue), the year 1999 (red), January to October 2000 (green), July to December 2001 (purple), and January to May 2002 (orange). The black curve corresponds to a moving average applied to the data, highlighting long-term trends.

This temporal analysis provides a better understanding of the marine dynamics at “Pointe de la Revellata” and their evolution over several years. It also shows the importance of high temporal resolution data to capture both rapid and long-term phenomena in complex coastal environments. Figure 31 shows a histogram of trends for current events exceeding 5 cm/s. The analysis reveals that in 1998, there were fewer than 10 strong current events, whereas in 2002, this number significantly increased, reaching a total of 60 events. This variation between the two years clearly illustrates the temporal variability of the currents on the same site.

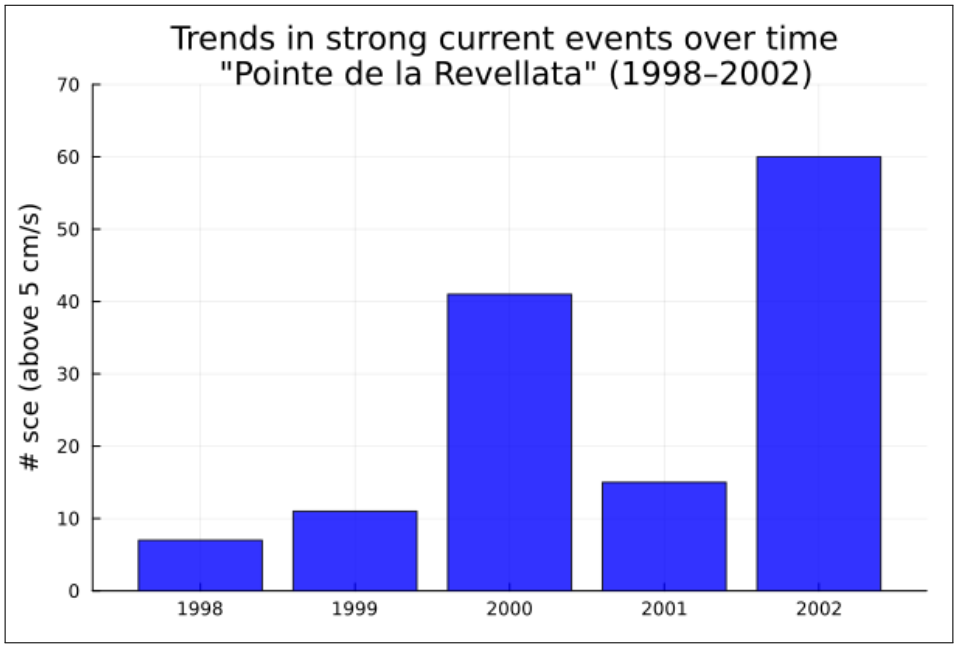

Figure 31: Strong currents events (SCE) recorded from 1998 to 2002 at the “Pointe de la Revellata” site.

3.3.2 Seasonal variations in currents

As demonstrated in the previous sections, there is clear spatial variability (both horizontal and vertical) in the currents, even on the same site. The currents are not uniform and vary depending on depth. This indicates both spatial and temporal variability. Additionally, we confirmed that winds are not the only drivers of currents in Calvi Bay. To illustrate these patterns, it is necessary to create maps that represent the same years, months, depths, and locations. However, few sites meet all these conditions. We use the Haida sites monitored during the 2016–2018 Haida campaign. These sites offer good spatial coverage, with samples collected monthly at each site, allowing for the creation of monthly maps for several years. The data includes samples from Haida sites 1 to 5 at a depth of 30 meters, and Haida sites 6 to 9 at a depth of 60 meters. There are no data for March, as no instruments were deployed during that month. Instead, the March map has been replaced with a site map, similar to figure 12, to show the locations of the various sampling points.

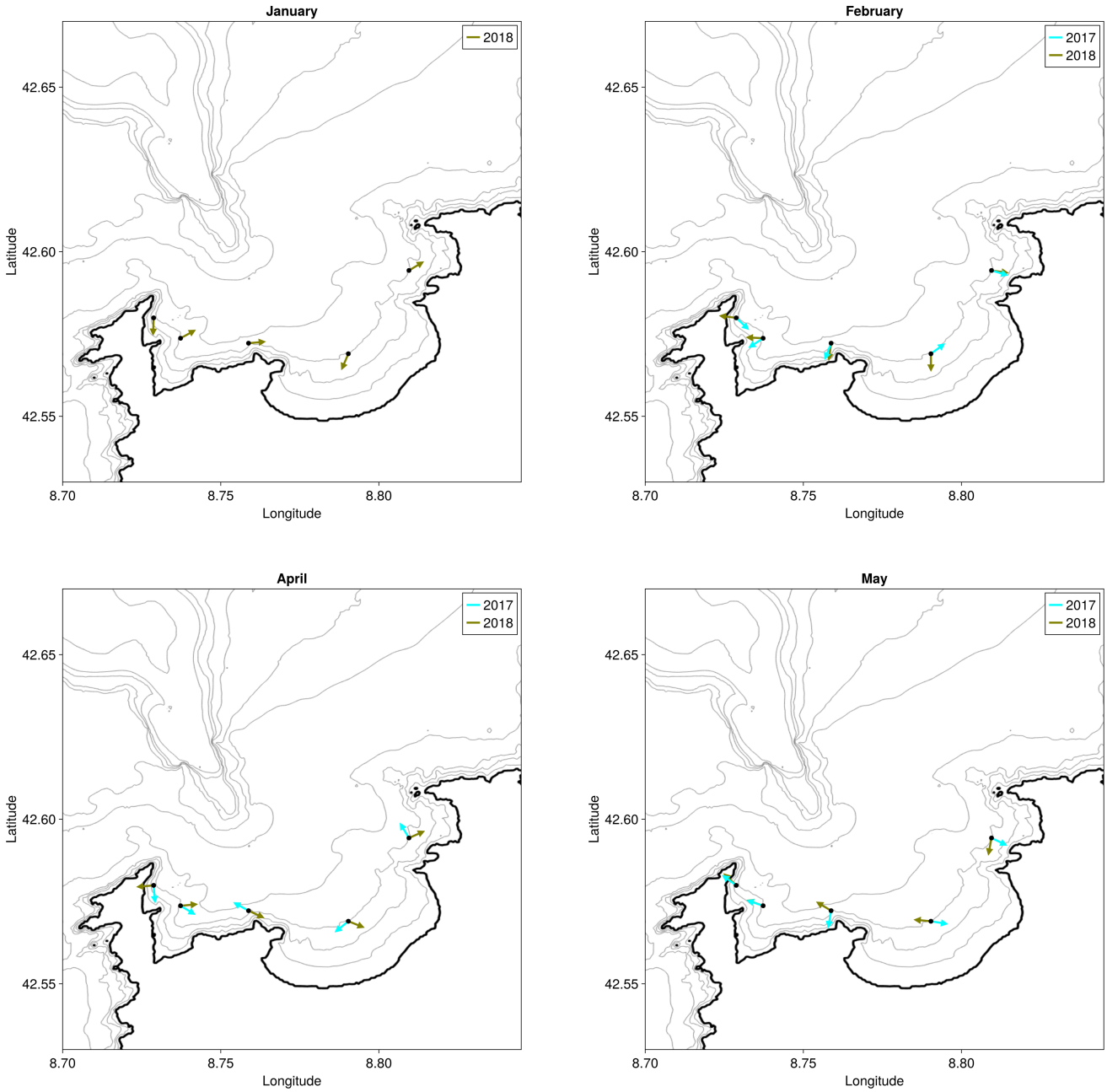

Figure 32: Monthly current maps from January to May, based on data from the Haida sites collected during the 2016–2018 campaign. Only the direction of the currents is represented. No significant data is available for March. Refer to figure 34 for the location of the different sites.

The current maps corresponding to the 30-meter depth, covering Haida sites 1 to 5, reveal diverse dynamics within the bay. Clear patterns emerge, with several sites exhibiting similar current directions. However, local phenomena at certain sites result in deviations from these shared trends. For instance, the map for September, shown in figure 33, highlights a well-defined flow: currents enter the bay from the northwest near Punta di Spanu, follow the coastline along Calvi Bay, traverse the Revellata Bay, and eventually reach Punta de la Revellata.

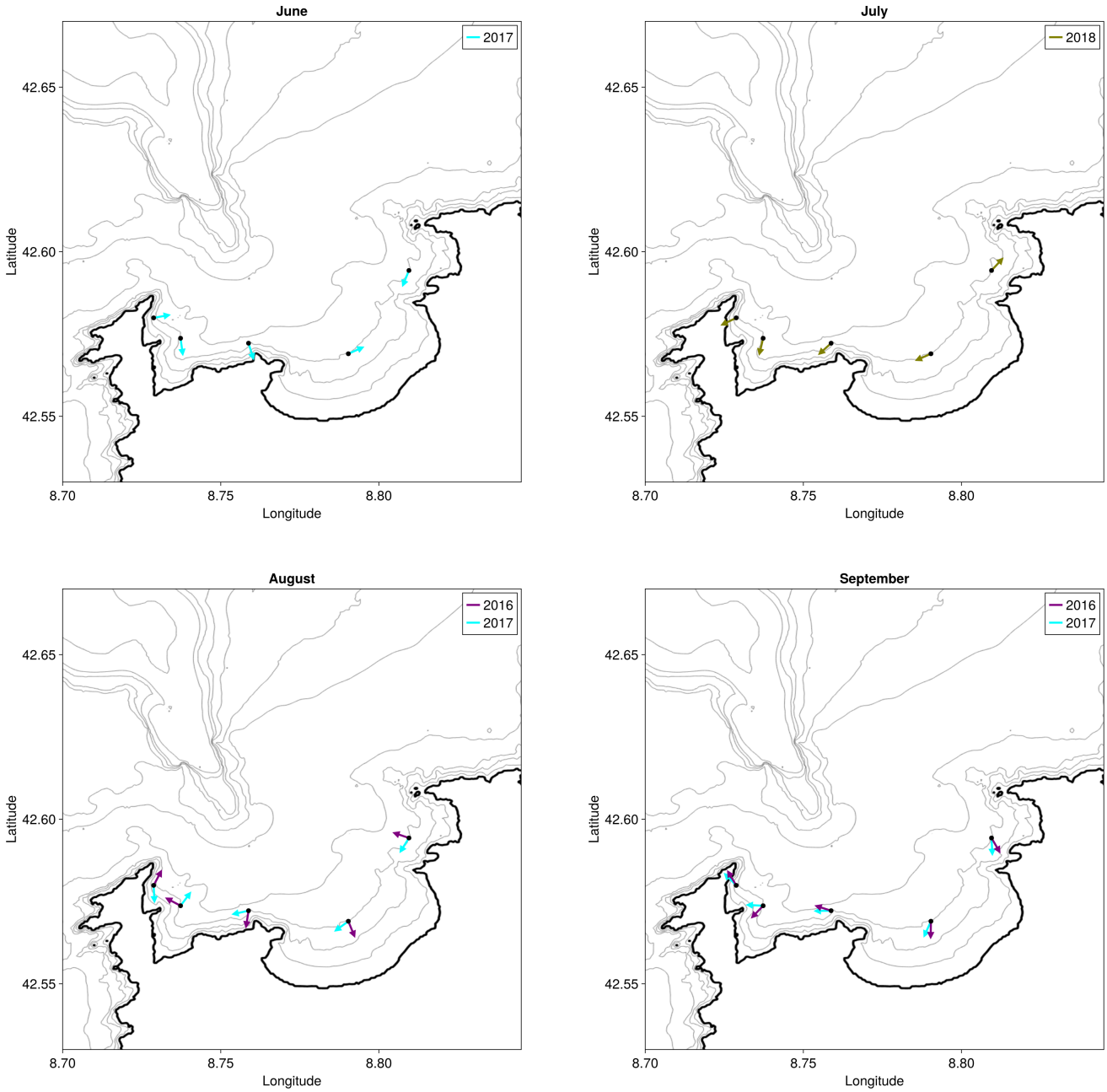

Figure 33: Monthly current maps from June to September, based on data from the Haida sites collected during the 2016–2018 campaign. Only the direction of the currents is represented. Refer to figure 34 for the location of the different sites.

An interesting feature is the variability observed from month to month, where the direction of circulation within the bay can change completely. This underlines the complexity of the hydrodynamic processes governing the area, influenced by both regional and local factors. For example, in April and May 2018, as shown in Figure 32, we can observe a clear change in the current direction. Except for the site near Punta de la Revellata, the currents in April tend towards Punta di Spanu, while in May, they shift towards Punta de la Revellata, indicating a complete reversal in the circulation pattern.

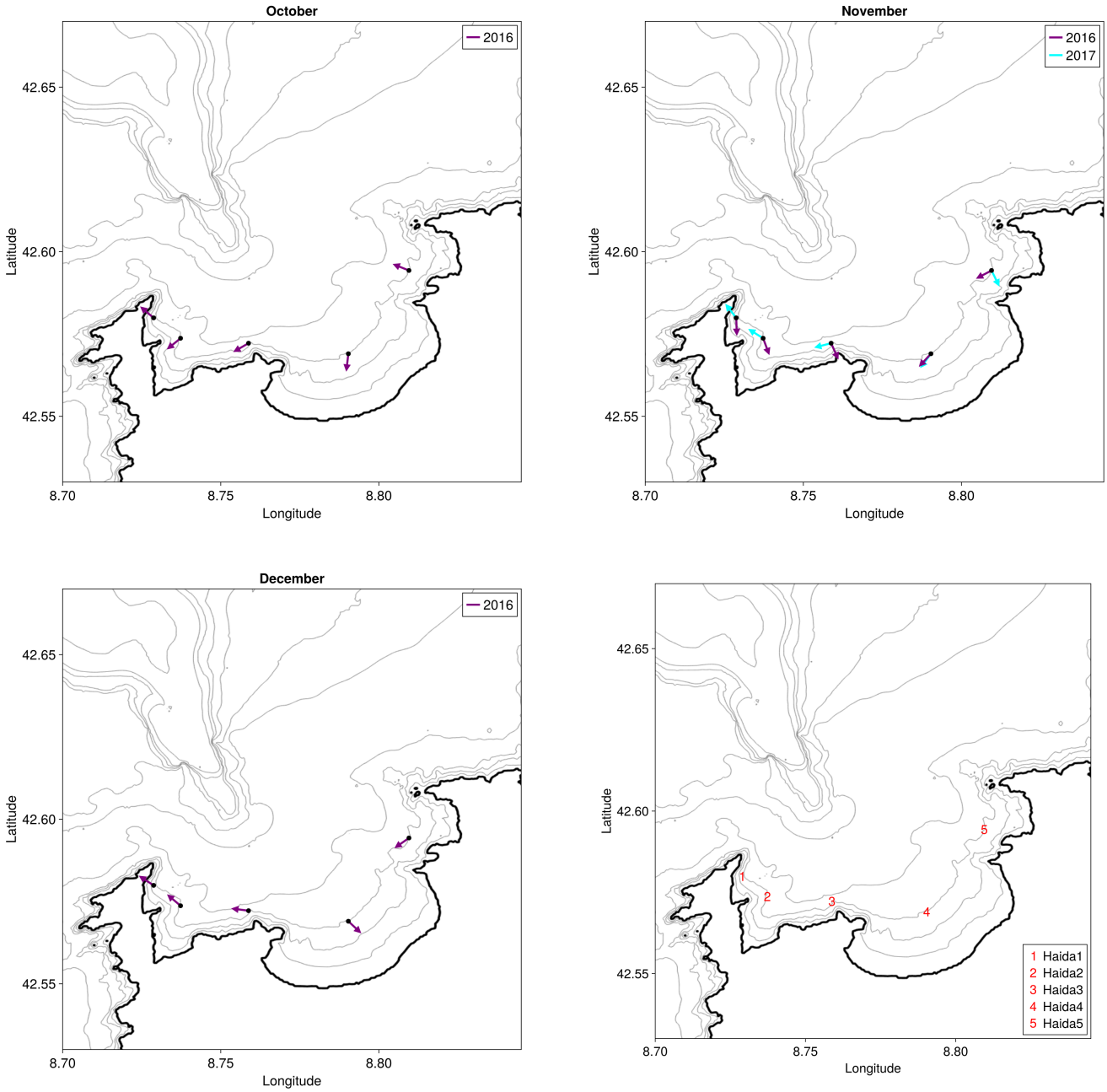

Figure 34: Monthly current maps from October to December, based on data from the Haida sites collected during the 2016–2018 campaign. Only the direction of the currents is represented. Refer to the last figure for the location of the different sites.

If we examine the output from the CORSE400 model (Figure 35), we can observe a similar dynamic pattern. This alignment between the model's results and the observed data reinforces the consistency of the hydrodynamic processes within the study area. Notably, the model data in figure 35 (a) also reveals the presence of an anticyclonic gyre (rotating clockwise), a structure previously mentioned in a study of the Bay of Calvi (Norro, 1995). Whereas figure 35 (b) gives a complete different dynamics. The model also shows us the impact of the WCC on Calvi Bay. Indeed, the modeling highlights the influence of this current on the local hydrodynamic dynamics, emphasizing its major role in the movement of the waters in the bay. The 60-meter depth maps can be found in the appendix for further reference (Figure 38).

The monthly current maps provide insights on the dynamics of the currents within the bay and their evolution throughout the year. By examining these maps, we can observe the seasonal variations in current patterns. These maps not only highlight the general trends but also reveal the changes in circulation and current intensities, giving a comprehensive view of the bay's dynamic behavior over time.

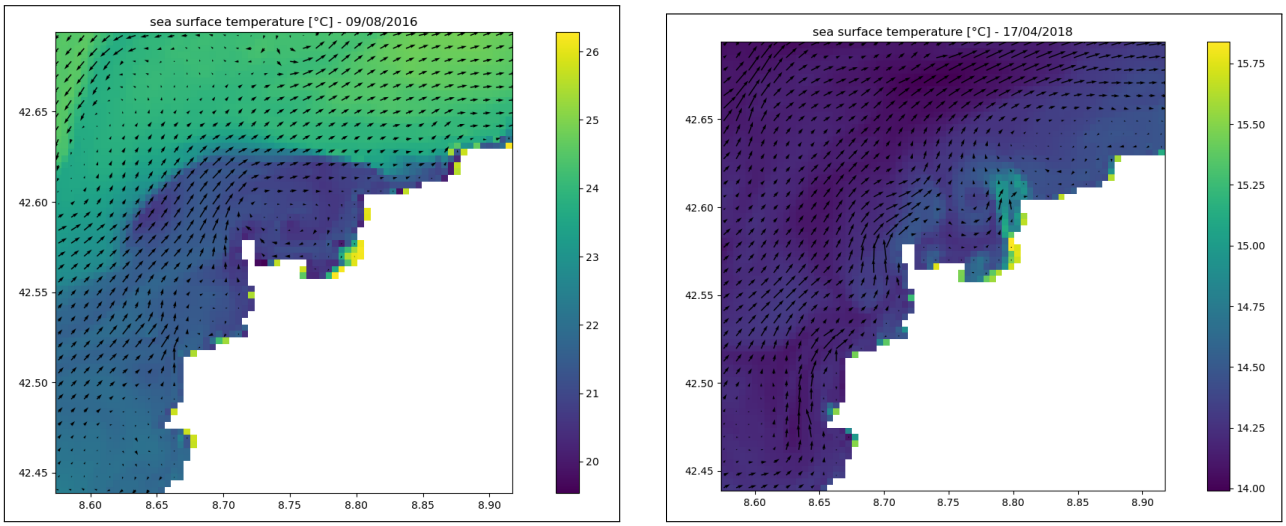

(a) (b)

Figure 35: Results from the CORSE400 model, showing SST(°C) in color and current speed (m/s) with arrows, (a) for August 9th, 2016, 6 a.m. and (b) for April 17th, 2018, 9 a.m.

4 Discussion

According to Poulain et al.(2012), wind has a significant influence on hydrodynamics in Corsica. However, our study analyzes the correlation between winds and currents and did not find similar results (tables 3 and 4). There were indeed issues with the data, as previously mentioned: the lower layer appeared to be more influenced by the winds than the upper layer, which is unexpected. Additionally, the profiles (figure 13) and vector time series (figure 14) from this study revealed a similar dynamic between currents and winds, converging with the findings of Poulain et al. (2012).

Norro (1995) identified the presence of several gyres during specific periods, highlighting their role in the hydrodynamics of the region. Using the monthly maps generated in this research (figure 32) and the CORSE400 model (figure 35), we were able to observe one of those gyres within Calvi Bay. This gyre exhibited an anticyclonic behavior, rotating clockwise, and appeared to influence the circulation patterns within the bay. The presence of this gyre aligns with the seasonal variability observed in the monthly maps. The CORSE400 model further corroborated this observation. Identifying this gyre does not only validate the earlier findings of Norro but also emphasizes the importance of mesoscale processes for the current dynamics of the bay. Future research could focus on quantifying the energy associated with such gyres and their potential ecological implications, on nutrient transport and biological productivity for example.

The frequency decomposition performed for the Pointe de la Revellata site in March revealed a process at 0.08 cycles per hour (figure 28) , a characteristic signature of tidal forces in Corsica. Furthermore, the low amplitude observed aligns with the known tidal behavior in Corsica. As highlighted by Colling (2001), energy peaks associated with tides can be detected in frequency decompositions. Therefore, it is plausible that the observed peak was caused by tidal currents. However, since no single process dominates the total energy distribution, this peak is likely also influenced by additional phenomena.

4.1 Methodological limitations and potential sources of error

Several limitations and potential sources of error were encountered throughout the study, which impacted the overall results.

One of the primary issues was with the export of CSV files from DataStudio 3D, the software of the constructor. Despite the data being correct, the CSV format was often corrupted, resulting in significant time spent refining and cleaning the data. This technical challenge delayed the analysis and complicated the process of working with the raw data and may be responsible for the error found in the Pearson's complex correlation.

Another limitation was the relatively small number of sites studied. The research would have benefitted from a broader spatial scope, which could provide a more representative understanding of the hydrodynamics across the entire Bay of Calvi. Thus, the time period covered by the measurements was limited. While the data gathered in 2023 offered valuable insights, extending the monitoring period would provide a better overview of long-term trends and variability in the region.

Issues with the deployment of instruments, including battery autonomy, also posed challenges. The lack of telemetry or loggers on the instruments made the monitoring of the the battery levels difficult. This led to gaps in data collection when the batteries were depleted. A more effective system, such as incorporating telemetry, would have allowed for the timely replacement of batteries and continuous monitoring throughout the campaigns. Errors with the third ADCP resulted in no data being collected from the "Pointe de Caldanu" site.

Having a single instrument on each site is often insufficient to obtain robust data and validate results. It would be ideal to have multiple instruments, in order to compare measurements. However, it is essential to take some precautions to avoid instruments from interfering with each other. Indeed, two ADCPs placed too close can interfere, affecting the quality of the data collected. To minimize this risk, it is recommended to space them a few meters apart or to use different acoustic frequencies for each instrument. Desynchronizing the pings of the instruments is advised, so that they do not emit acoustic waves at the same time. By following these practices, it is possible to better rely on the measurements while using multiple instruments on the same site.

The data processing was suffering from a lack of standardization. In some cases, data files were missing essential information such as date, longitude, latitude, or depth. Without proper headers or consistent formatting, consolidating data from different sources was a cumbersome and time-consuming task. A more standardized approach to data collection and organization would have greatly facilitated data analysis.

The lack of a centralized platform for data management made it difficult to integrate and access all available datasets. Although the RACE database would serve as a useful tool for centralizing data, not all of the datasets are included in it, which complicates the process of retrieving and combining relevant data from various sources.

4.2 Improvements and future research suggestions

To enhance the methodology for measuring currents in the Bay of Calvi, several improvements can be suggested. First, increasing the number of sampling sites would provide a more comprehensive spatial coverage, allowing for a better understanding of the bay's hydrodynamics. Extending the study periods would help capture longer-term variations and trends, improving the reliability of the data. Adjusting the sampling frequency to every hour instead of every 30 minutes could help preserve the instruments' battery life and extend the duration of data collection.

Making specific recommendations to the STARESO scientific base, which has recently acquired a new boat equipped with ADCP, could significantly benefit future research. Providing detailed guidelines on the proper calibration and parameterization of the ADCP would ensure accurate and high-quality data collection, maximizing the potential of this advanced equipment. By implementing these suggestions, future studies could achieve more robust and comprehensive results, enhancing our understanding of the bay's current dynamics.

Figure 36: One of the 2024 drifters, made by the Liège oceanography master students and used to measure surface currents in the Bay of Calvi.

In 2023 and 2024, with the support of Aïda Alvera-Azcarate and Alexander Barth, first-year master's students in oceanography at the University of Liège constructed drifters to estimate surface currents and SST in the bay. Each drifter was equipped with a Raspberry Pi, logging GPS coordinates, and a temperature sensor. In May 2023, five drifters were deployed, followed by ten more in May 2024. Drifters give insights on the current surface, which is difficult to estimate using ADCPs set at the bottom of the ocean. This difficulty results from the back-scattering of the water surface, which can interfere with the ADCPs' currents surface measurements. The use of drifters improves our currents measurement in the water column, giving a better understanding of the bay hydrodynamics. These drifters were deployed for 2 days. This deployment captured hydrodynamic data for a period and a location not covered by previous campaigns.

5 Conclusion

This study provided an in-depth exploration of the currents dynamics in the Bay of Calvi through a combination of field measurements and analysis of historical data. By integrating different methodologies, we were able to observe current variations and analyze their relationship with local meteorological conditions. This section summarizes the key findings, discusses their implications for the understanding of the region, and offers recommendations for future research and marine resource management.

5.1 Summary of the study

This study aimed to investigate the hydrodynamic processes in the Bay of Calvi by combining field measurements and meta-analysis of historical data. Four measurement campaigns were conducted across two sites, using an Acoustic Doppler Current Profiler (ADCP) to capture high-resolution current data. Understanding the functioning and proper parameterization of the ADCP was crucial for obtaining accurate measurements. The field data, collected in 2023, were compared with historical data from previous years, providing valuable insights into long-term trends and changes in the bay's hydrodynamics. By combining both contemporary measurements and historical data, the study improves our understanding of the interactions between oceanographic / atmospheric processes and current dynamics. The findings contribute significantly to the comprehension of the region's marine environment, with potential applications in resource management and environmental monitoring. This research highlights key factors influencing the bay's circulation and provides important perspectives for future studies in the area.

5.2 Synthesis of major findings of the study

This study aimed to investigate the currents in Calvi Bay by deploying ADCP instruments at two different sites and revisiting historical data from 1998 to 2002 and 2016 to 2018. Through the creation of current profiles, the identification of general trends as well as spatial and temporal variability has been done. These profiles also led to the discovery of an atmospheric front, providing further insight into the region's dynamic conditions.

In addition, vector time series associated with wind data revealed a moderate correlation between winds and currents. By extracting the mean and standard deviation of the u and v components, it has been observed that intermediate waters responded differently to wind forces compared to surface or deep waters. A Pearson's complex correlation analysis explored the strength of the wind-current relationship, although some errors did affect the results.

Frequency decomposition analysis helped to uncover large-scale, low-frequency phenomena that influence the currents, and also allowed for the identification of tidal effects. To trace the evolution of currents over time, the creation of time-series profiles from 1998 to 2002, shows significant variability, alongside histograms highlighting periods of high current events on the same site.

For a deeper understanding of seasonal changes, monthly maps from 2016 to 2018 were generated, illustrating the dynamic evolution of the currents over several years. To validate these findings, the CORSE400 model has been used, which not only confirmed the observed patterns but also highlighted the presence of a gyre within the bay, further solidifying the study's conclusions.

5.3 Resolving the research questions

5.3.1 Temporal and spatial variations of the currents in Calvi Bay

The study of the currents in Calvi Bay reveals both spatial and temporal variations, which are influenced by a combination of local and regional hydrodynamic factors. Spatial variability is particularly evident when comparing different observation sites, such as the "Pointe de la Revellata", "Baie de Calvi" and other Haida sites across the bay. These sites show distinct current behaviors, with different directions and intensities, which highlight the diverse hydrodynamic conditions within the bay. Furthermore, the depth also plays a critical role in the variation of current dynamics. At 30 meters, significant differences in current direction are observed compared to shallower layers, with the currents in deeper regions potentially being more affected by larger-scale oceanographic processes.

The temporal variability of the currents also shows distinct patterns across different months, as reflected in the monthly current maps. The currents exhibit major directional shifts between April and May, with the direction changing from Punta de Spano to Punta de la Revellata, illustrating strong seasonal effects. These shifts can be attributed to changing wind patterns, an influence of the WCC, or large-scale processes. This seasonal variation in currents supports the hypothesis of the bay's complex hydrodynamics, where different factors interact to alter the direction and intensity of currents over the year.

5.3.2 Main dynamics of the currents in Calvi Bay and their evolution across the different periods

The main dynamics of the currents in Calvi Bay are characterized by a complex interplay of local, regional, and seasonal influences. From the 2016–2018 Haida data and the CORSE400 model, we observe recurring patterns, including gyres that shape the overall circulation within the bay. A prominent feature identified is the cyclonic and anticyclonic gyres, which have been reported in previous studies (Norro, 1995), and are consistently observed in both the model and the observed data.

Looking at the data across several periods (1998–2002, 2015–2018, and 2023–2024) shows that the main dynamics of the currents have remained relatively stable over time, with some seasonal and annual variations. However, the more recent data, particularly from 2023–2024, shows a slight shift in current behavior, possibly indicating the influence of ongoing changes in the regional climate, such as warming waters.

The spatial coverage of the Haida sites, with monthly samples from each site, provides a broader understanding of these dynamics, highlighting how different parts of the bay experience varied current behaviors at different times of the year. Additionally, the model outputs from CORSE400 confirm these observed trends. This agreement between the observed data and model simulations strengthens the reliability of the study.

In summary, the analysis of both the observed and modeled data has allowed us to better understand the current dynamics in Calvi Bay and how it evolvs across different periods. However, some areas remain unclear. For instance, while we have identified large-scale processes through the frequency decomposition of the u and v components (figure 26, 27 and 28), we still need to understand which processes produce these energy peaks. Moreover, we do not fully understand the exact factors driving the variability observed in the standard deviation at intermediate depths (figure 19 and 25). Further investigations are needed to reveal the specific mechanisms behind these variations and to refine our understanding of the bay's complex hydrodynamics.

5.4 Implications and recommendations

The findings of this study provide insights about the hydrodynamics of the Bay of Calvi and open up several avenues for further investigation. While the study has contributed to our understanding of the current dynamics, it also highlights areas where improvements can be made in terms of data collection, analysis, and long-term monitoring. The following sections give an overview of key recommendations for future research, suggestions for improving methodologies, and the potential implications of the study's findings for marine resource management. These recommendations aim to improve the scientific understanding of the region's hydrodynamics and support the sustainable management of its marine resources.

5.4.1 Recommendations for future research

The field data collected over several campaigns have revealed interesting trends, but one of the key recommendations is to improve the temporal and spatial resolution of measurements.

The "Pointe de la Revellata" site has been frequently referenced throughout this study, as it has been extensively monitored during several campaigns. However, to gain a more comprehensive understanding of the bay's hydrodynamic processes, it would be interesting to expand the research to other sites within the area. This broader approach could help to capture the full spectrum of the bay's dynamics. Increasing the frequency of measurements, particularly during extreme weather conditions, would provide a better understanding of the short-term variability of currents.

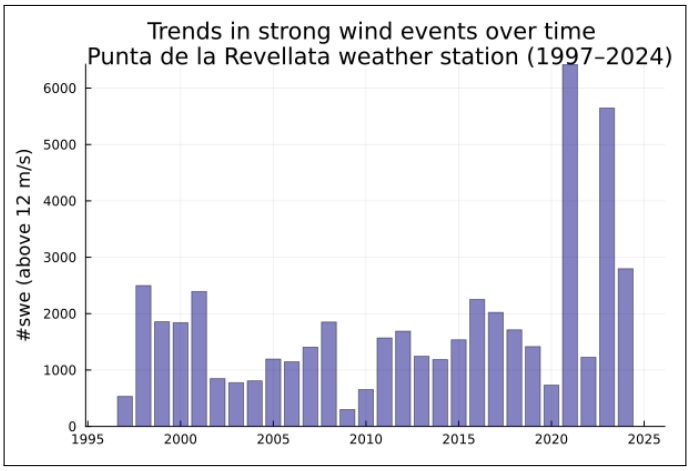

Figure 37: Strong wind events (SWE) recorded from 1997 to 2024 at the weather station situated in Punta de la Revellata. This figure was created to verify if SWE were more frequent today than 30 years ago. The figures show an important amount of events in 2021 and 2023.

Future research could focus on the long-term impacts of climate change on the Bay of Calvi, particularly regarding water warming, changes in wind patterns, and the increasing frequency of strong wind events (figure 37). As these events are expected to become more frequent and intense due to climate change, studying their effects could help to identify any shifts in hydrodynamic processes.

To gain a deeper understanding of the evolving dynamics in the region, the establishment of continuous monitoring stations is also recommended. These stations would enable the collection of real-time data, allowing for a more comprehensive view of the short-term fluctuations and long-term changes in the currents of the bay. This of course, would be complicated to implement, as the area is designated for anchoring, and there is a risk that some individuals would take the equipment.

A more realistic approach could involve combining remote sensing and machine learning. By automating the detection of structures in real-time satellite data (or data from the past week), it would become easier to precisely identify the best locations for deploying monitoring instruments. For example, some coordinates often show the formation of a front, which would be an ideal spot for establishing a new site. The integration of AI would help to automatize the work of researchers, allowing them to focus more on the most significant aspects of the study. Many recent studies focus on this topic (Meng and Yan, 2022,

Song et al., 2023, H. Wang and Li, 2023).

This study has contributed to the organization and reformatting of historical data, making it easier to analyze. By carefully reviewing, structuring these past datasets, and creating scripts to access meteorological data, or creating figures, they can now be more effectively integrated into future studies, providing a valuable resource for ongoing research in the region.

5.4.2 Suggestions for improved methodologies

One important area for improvement lies in increasing the spatial and temporal resolution of measurements. The more measurement points we have, the better we can understand the dynamics of currents. This would allow for a more precise identification of complex phenomena, such as gyres. While satellite data can be used for such analysis, they are often affected by cloud coverage and mainly give surface dynamics of the water masses. More frequent campaigns with better spatial coverage would provide a more detailed view of the currents in the bay.

In this regard, the new boat equipped with an ADCP at STARESO presents an excellent opportunity to increase the frequency of measurements and facilitate the study of the global dynamics of currents. This would reduce delays due to weather conditions and also offer better instrument autonomy, as the technical issues related to non-rechargeable batteries encountered in this study has been critical. The use of ADCPs better suited to shallow waters, as opposed to those originally designed for greater depths, would be beneficial. Newer ADCPs come with up-to-date software suites and modern file systems, which would make them easier to use. In this study, processing the .data files was challenging, as this file format is not very widespread. The manufacturer's software could read them, but resulted in erroneous CSV files (e.g., duplicate lines or the inability to extract specific columns). These issues caused time delays and complications in data analysis.

Regarding historical data, several issues were encountered. Some data were in incorrect formats, others were incomplete, and some lacked headers, complicating their processing and analysis. Additionally, these data are not centralized, and although the RACE database is perfect to host them, this is not always the case. Harmonization of the data is needed, with standardized formats adopted across the datasets. For example, it would be helpful to have uniform headers for each dataset, as well as CSV files with columns having the same names, to simplify their processing. An associated text file for each dataset could detail the specifics of each campaign: the sites studied, the depth, the instruments used, and the availability of auxiliary data (such as atmospheric conditions or water temperature). This organization would make the data more accessible and easier to process in the long term.

Furthermore, the use of additional instruments could significantly enhance the accuracy and scope of future studies. For example, some past campaigns utilized satellite-tracked drifters to study surface currents (Ohshima et al., 2002, Chaigneau and Pizarro, 2005), which remains a major gap in the current study. Due to issues with back-scattering, surface current data was not available, thus limiting our understanding on surface dynamics. Incorporating such drifters or other surface measurement tools in future campaigns would be invaluable to fill this data gaps and provide a more complete picture of the circulation dynamics.

5.4.3 Implications for marine resource management

While the primary focus of this study was to advance our understanding of the hydrodynamics in the Bay of Calvi, the data collected and organized could also serve as a valuable resource for local resource management. Though not the main priority, these data provide insights into the region's current dynamics, which could help inform decision-making processes related to marine conservation, coastal development, and climate adaptation strategies. For example, the patterns of current variability and their relationship with meteorological conditions could assist in optimizing the placement of marine structures or monitor the health of sensitive ecosystems. By making these data more accessible, this study could contribute to a more data-driven approach in managing the bay's marine environment.

6 References

Ahumada, M., & Cruzado, A. (2007). Modeling of the circulation in the northwestern mediterranean sea with the princeton ocean model. *Ocean Science*, *3*(1), 77–89. https://doi.org/https://doi.org/10.5194/os-3-77-2007

Astraldi, M., Gasparini, G., Manzella, G., & Hopkins, T. (1990). Temporal variability of currents in the eastern Ligurian sea. *Journal of Geophysical Research: Oceans*, *95*(C2), 1515–1522.

Astraldi, M., Gasparini, G. P., & Sparnocchia, S. (1994). The seasonal and interannual variability in the ligurian-provençal basin. *Seasonal and interannual variability of the Western Mediterranean Sea*, *46*, 93–113. https://doi.org/https://doi.org/10.1029/CE046p0093

Barth, A., Alvera-Azcárate, A., Rixen, M., & Beckers, J.-M. (2005). Two-way nested model of mesoscale circulation features in the ligurian sea. *Progress in Oceanography*, *66*(2-4), 171–189. https://doi.org/10.1016/j.pocean.2004.07.017

Beesley, D., Olejarz, J., Tandon, A., & Marshall, J. (2008). A laboratory demonstration of coriolis effects on wind-driven ocean currents. *Oceanography*, *21*(2), 72–76. https://doi.org/https://www.jstor.org/stable/24805614

Chaigneau, A., & Pizarro, O. (2005). Mean surface circulation and mesoscale turbulent flow characteristics in the eastern south pacific from satellite tracked drifters. *Journal of Geophysical Research: Oceans*, *110*(C5). https://doi.org/10.1029/2004JC002628

Colling, A. (2001). *Ocean circulation* (Vol. 3). Butterworth-Heinemann. https://books.google.fr/books?hl=fr&lr=&id=QjBbuwZ15uYC&oi=fnd&pg=PA8&dq=ocean+circulation+angela+colling&ots=Xy7elPOlO0&sig=-E7-s70PvGQfuEy5rTd0yH4y_ps&redir_esc=y#v=onepage&q=ocean%20circulation%20angela%20colling&f=false

de La Faverie du Ché, C.-H. (2019). *Arrete prefectoral n°123/2019*. https://www.premar-mediterranee.gouv.fr/uploads/mediterranee/arretes/eec503812bac663e9c5536c6d5a59ee1.pdf

Echevin, V., Crepon, M., & Mortier, L. (2003). Interaction of a coastal current with a gulf: Application to the shelf circulation of the gulf of lions in the mediterranean sea. *Journal of physical oceanography*, *33*(1), 188–206. https://doi.org/https://doi.org/10.1175/1520-0485(2003)033⟨0188:IOACCW⟩2.0.CO;2

Elliott, A. (1979). Effect of low-frequency winds on sea-level and currents in the gulf of genova. *Oceanologica Acta*, *2*(4), 429–433. https://archimer.ifremer.fr/doc/00122/23359/21186.pdf

Gobert, S., Lejeune, P., Marengo, M., Donnay, A., & Leduc, M. (2018). *Starecapmed, rapport d'activité 2017*. STARESO, Calvi, France. https://doi.org/https://hdl.handle.net/2268/229667

Goffart, A., Hecq, J.-H., & Legendre, L. (2002). Changes in the development of the winter-spring phytoplankton bloom in the bay of Calvi (NW Mediterranean) over the last two decades: A response to changing climate? *Marine Ecology Progress Series*, *236*, 45–60. https://doi.org/10.3354/meps236045

Gonella, J. (1972). A rotary-component method for analysing meteorological and oceanographic vector time series. *Deep Sea Research and Oceanographic Abstracts*, *19*(12), 833–846. https://doi.org/10.1016/0011-7471(72)90002-2

Gregorius, T., & Blewitt, G. (1998). The effect of weather fronts on gps measurements. *GPS world*, *9*(5), 52–60. https://api.semanticscholar.org/CorpusID:15765597

Kostaschuk, R., Best, J., Villard, P., Peakall, J., & Franklin, M. (2005). Measuring flow velocity and sediment transport with an Acoustic Doppler Current Profiler. *Geomorphology*, *68*(1-2), 25–37. https://doi.org/https://doi.org/10.1016/j.geomorph.2004.07.012

Law, K. L., Morét-Ferguson, S., Maximenko, N. A., Proskurowski, G., Peacock, E. E., Hafner, J., & Reddy, C. M. (2010). Plastic accumulation in the north atlantic subtropical gyre. *Science*, *329*(5996), 1185–1188. https://doi.org/10.1126/science.1192321

Lepoint, G. (2001). *Compétition pour l'azote inorganique entre le pelagos et le benthos dans un écosystème côtier oligotrophe. effets sur la dynamique de l'écosystème.* [Doctoral dissertation, ULiège-Université de Liège]. https://doi.org/https://hdl.handle.net/2268/27264

Meng, L., & Yan, X.-H. (2022). Remote sensing for subsurface and deeper oceans: An overview and a future outlook. *IEEE Geoscience and remote sensing magazine*, *10*(3), 72–92. 10.1109/MGRS.2022.3184951

Minobe, S., Kuwano-Yoshida, A., Komori, N., Xie, S.-P., & Small, R. J. (2008). Influence of the gulf stream on the troposphere. *Nature*, *452*(7184), 206–209. https://doi.org/https://doi.org/10.1038/nature06690

Moebs, W., J. Ling, S., & Sanny, J. (2023). University physics, volume one. Independently Published. https://pressbooks.online.ucf.edu/osuniversityphysics/chapter/17-7-the-doppler-effect/

Norro, A. (1995). Etude pluridisciplinaire d'un milieu côtier. approches expérimentale et de modelisation de la baie de calvi (corse). *Th Doctorat Univ Liège Belgique*, *258*.

Nortek. (2021). *Understanding adcps*. Nortek. https://www.nortekgroup.com/knowledge-center/wiki/guide-to-understanding-adcps

Ohshima, K. I., Wakatsuchi, M., Fukamachi, Y., & Mizuta, G. (2002). Near-surface circulation and tidal currents of the okhotsk sea observed with satellite-tracked drifters. *Journal of Geophysical Research: Oceans*, *107*(C11), 16–1. https://doi.org/10.1029/2001JC001005

Poulain, P., Gerin, R., Rixen, M., Zanasca, P., Teixeira, J., Griffa, A., Molcard, A., De Marte, M., & Pinardi, N. (2012). Aspects of the surface circulation in the Liguro-Provencal basin and Gulf of Lion as observed by satellite-tracked drifters (2007-2009). *Bollettino di Geofisica Teorica e Applicata*, *53*(2), 261–279. https://doi.org/10.4430/bgta0052

Remy, F. (2016). *Characterization, dynamics and trophic ecology of macrofauna associated to seagrass macrophytodetritus accumulations (calvi bay, mediterranean sea)* [Doctoral dissertation, ULiège-Université de Liège]. https://doi.org/https://hdl.handle.net/2268/195829

Richir, J., Abadie, A., Binard, M., Biondo, R., Boissery, P., Borges, A., Cimiterra, N., Collignon, A., Champenois, W., Donnay, A., et al. (2015). Starecapmed (station of reference and research on change of local and global anthropogenic pressures on mediterranean ecosystems drifts)-année 2014. rapport de recherches. https://hdl.handle.net/2268/187710

Schroeder, K., Garcia-Lafuente, J., Josey, S. A., Artale, V., Nardelli, B. B., Carrillo, A., Gacic, M., Gasparini, G. P., Herrmann, M., Lionello, P., et al. (2012). Circulation of the mediterranean sea and its variability. *The climate of the Mediterranean region*, *187*. https://www.researchgate.net/profile/Emil-Stanev/publication/250928260_Circulation_Of_The_Mediterranean_Sea_And_Its_Variability/links/575740c208ae05c1ec16d16e/Circulation-Of-The-Mediterranean-Sea-And-Its-Variability

Skliris, N., Goffart, A., Hecq, J.-H., & Djenidi, S. (2001). Shelf-slope exchanges associated with a steep submarine canyon off Calvi (Corsica, NW Mediterranean sea): A modeling approach. *Journal of Geophysical Research: Oceans*, *106*(C9), 19883–19901. https://doi.org/https://doi.org/10.1029/2000JC000534

Skliris, N., Hecq, J.-H., & Djenidi, S. (2002). Water fluxes at an ocean margin in the presence of a submarine canyon. *Journal of Marine Systems*, *32*(1-3), 239–251.

Song, T., Pang, C., Hou, B., Xu, G., Xue, J., Sun, H., & Meng, F. (2023). A review of artificial intelligence in marine science. *Frontiers in Earth Science*, *11*, 1090185. https://doi.org/10.3389/feart.2023.1090185

Šverko, Z., Vrankić, M., Vlahinić, S., & Rogelj, P. (2022). Complex pearson correlation coefficient for eeg connectivity analysis. *Sensors*, *22*(4), 1477. https://doi.org/10.3390/s22041477

Urone, P. P., & Hinrichs, R. (2020). Physics. OpenStax. https://archive.org/search.php?query=external-identifier%3A%22urn%3Aoclc%3Arecord%3A1391283554%22

Van Rijn, L. C. (2007). Unified view of sediment transport by currents and waves. ii: Suspended transport. *Journal of hydraulic Engineering*, *133*(6), 668–689. https://doi.org/https://doi.org/10.1061/(ASCE)0733-9429(2007)133:6(668)

Viollette, L. (1994). *Seasonal and interannual variability of the western mediterranean sea*. American Geophysical Union.

Wang, D., Wang, H., Li, M., Liu, G., & Wu, X. (2013). Role of ekman transport versus ekman pumping in driving summer upwelling in the south china sea. *Journal of Ocean University of China*, *12*, 355–365. https://doi.org/https://doi.org/10.1007/s11802-013-1904-7

Wang, H., & Li, X. (2023). Deepblue: Advanced convolutional neural network applications for ocean remote sensing. *IEEE Geoscience and Remote Sensing Magazine*. 10.1109/MGRS.2023.3343623

Williams, R. G., & Follows, M. J. (2003). Physical transport of nutrients and the maintenance of biological production. In *Ocean biogeochemistry: The role of the ocean carbon cycle in global change* (pp. 19–51). Springer. https://doi.org/10.1007/978-3-642-55844-3_3

Zhang, R., Xu, X., Gu, L., Tao, Y., & Wu, J. (2017). The influence of bottlenose dolphin (tursiops truncatus) click signal on the performance of underwater acoustic instruments, 1–5. https://10.1109/ICSPCC.2017.8242594

7 Appendix

7.1 Additional data

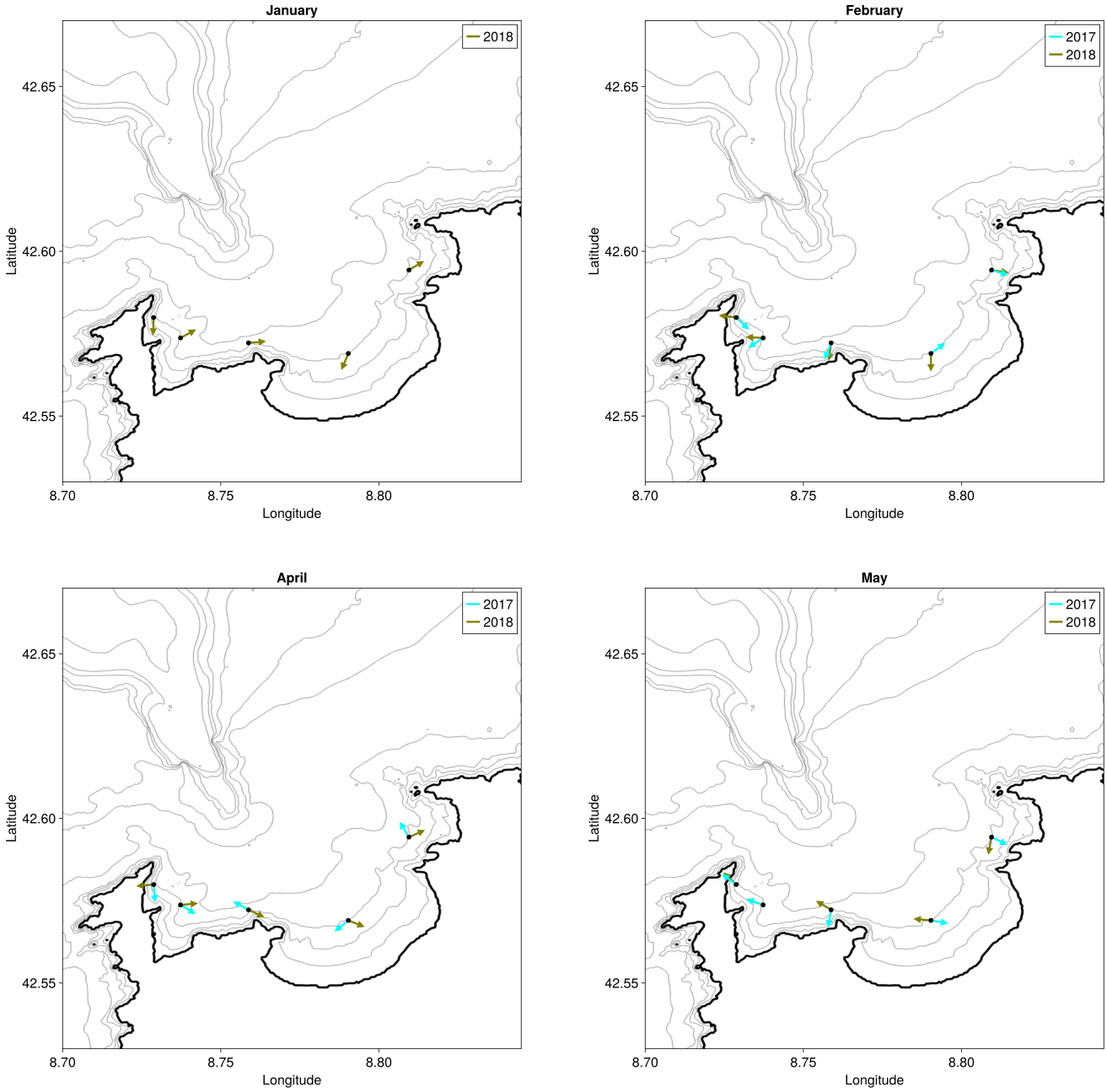

Figure 38: Monthly current maps from January to May, based on data from the Haida sites collected during the 2016–2018 campaign at 60 meters depth. Only the direction of the currents is represented. No significant data is available for March. Refer to figure 34 for the location of the different sites.

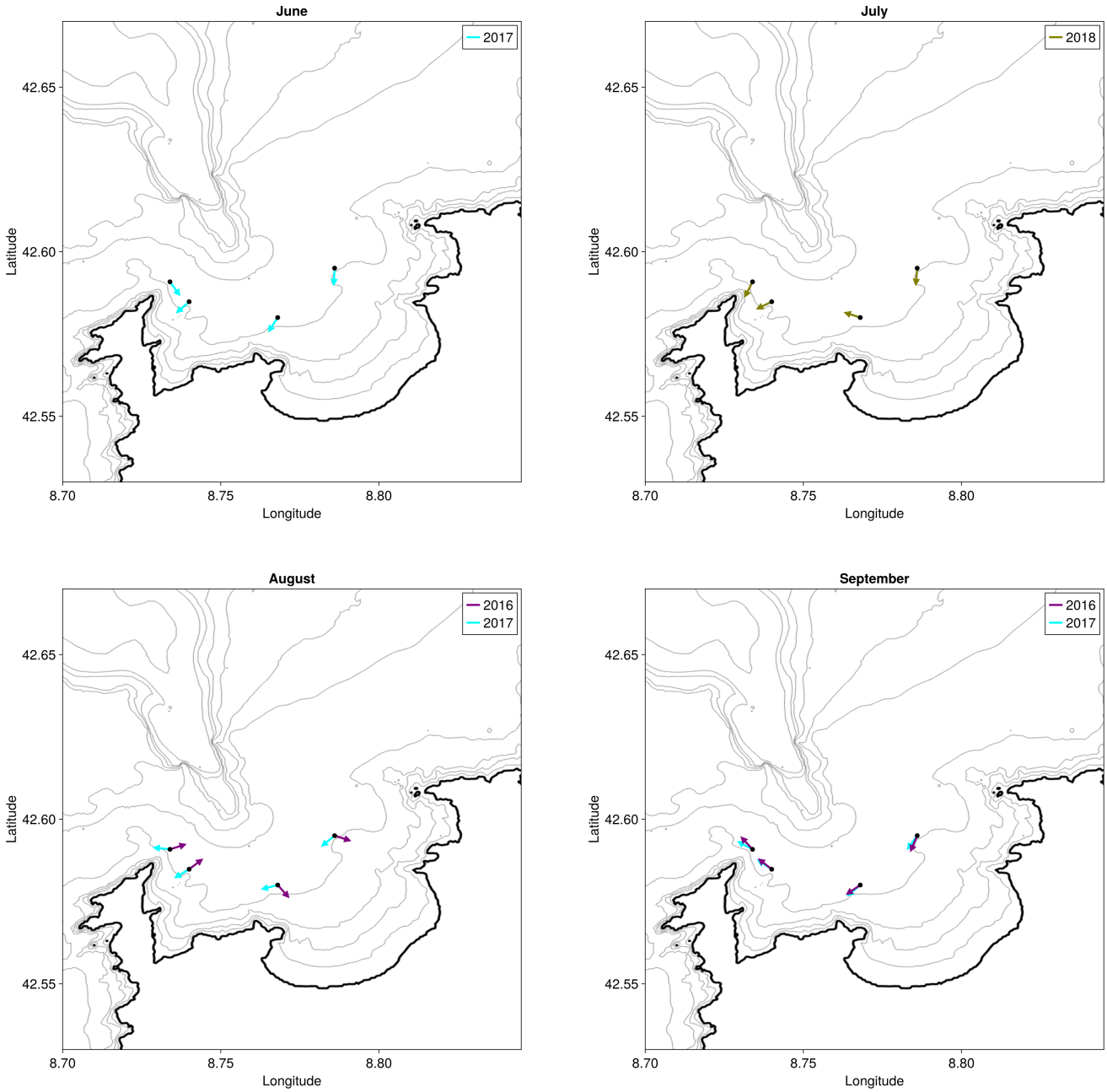

Figure 39: Monthly current maps from June to September, based on data from the Haida sites collected during the 2016–2018 campaign at 60 meters depth. Only the direction of the currents is represented. Refer to figure 40 for the location of the different sites.

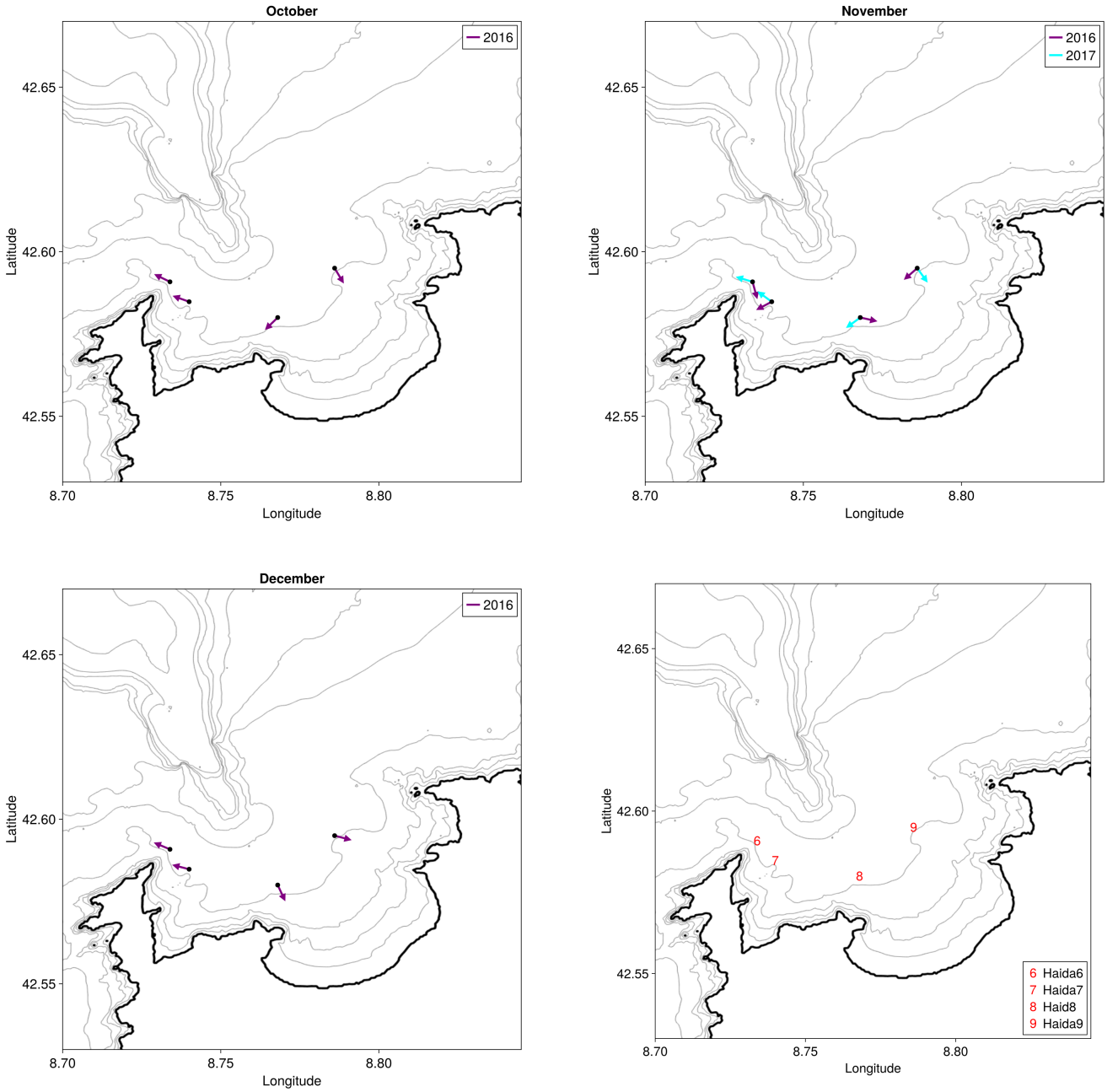

Figure 40: Monthly current maps from October to December, based on data from the Haida sites collected during the 2016–2018 campaign at 60 meters depth. Only the direction of the currents is represented. Refer to the last figure for the location of the different sites.

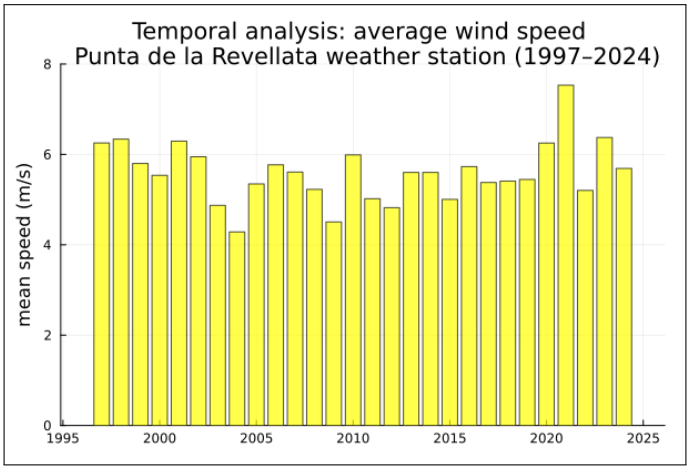

Figure 41: Average wind speed recorded from 1997 to 2024 at the weather station situated in Punta de la Revellata. This figure was generated to verify if the wind speed was increasing through the years. Data show that wind speed is consistent from 1997 to 2024, with higher values in 2021. The same event is shown in figure 37.